Supporting Information for:

Protonation and Concerted Proton-Electron Transfer Reactivity of a Bis-Benzimidazolate Ligated [2Fe-2S] Model for Rieske Clusters

Caroline T. Saouma, Werner Kaminsky, James M. Mayer*

Department of Chemistry, University of Washington, Box 351700, Seattle, WA 98195-1700, U.S.A.

Table of Contents

General Considerations**……..……..S-3**

Spectroscopic Measurements**.....S-3**

X-ray Crystallography Procedures **.....S-4**

Figure S1. Thermal ellipsoid (50%) representation of the core atoms of **1** and **2**……...**S-5**

Starting Materials and Reagents **.....S-6**

Synthesis of Clusters **.....S-6**

Figure S2. ^{1}H NMR spectrum of **1** (MeCN-d_3, 25 ^{o}C) **.....S-9**

Figure S3. ^{1}H/^{1}H COSY spectrum of **1** (DMF-d_7, 25 ^{o}C)**.....S-10**

Figure S4. ^{1}H NMR spectrum of **2** (MeCN-d_3, 25 ^{o}C).. **.....S-11**

Figure S5. ^{1}H/^{1}H COSY spectrum of **2** (MeCN-d_3, 25 ^{o}C)**.....S-12**

Figure S6. ^{1}H NMR spectrum (MeCN-d_3, 25 ^{o}C) of *in situ* generated **3.** **.....S-13**

Figure S7. Plot of chemical shift (Ar-H) *vs.* equiv acid ([pyH]OTf) added to **1** **.....S-14**

Figure S8. ^{1}H NMR spectra (MeCN-d_3, –20 ^{o}C) of *in situ* generated **4.** **.....S-15**

Figure S9. Stacked ^{1}H NMR spectrum (MeCN-d_3, -20 ^{o}C) of **2**/**4** showing reversibility **.....S-16**

Figure S10. UV-vis spectra of **1** and **2** in MeCN**.....S-17**

Figure S11. Stacked UV-vis spectra (MeCN) of **1** in the presence of acid then base.. **.....S-18**

Figure S12. Stacked UV-vis spectra (MeCN, –20 ^{o}C) of **2** with increasing amounts of acid **..S-19**

Figure S13. EPR spectrum of **2**.....**S-20**

Figure S14. Stacked IR spectra (KBr) of **H-3** and **D-3**.....**S-21**

Reaction of 4 with oxidants. **.....S-22**

Figure S15. Stacked ^{1}H NMR spectra (MeCN-d_3) showing the reaction of **4** with TEMPO **...S-23**

pK_a Determination of [Fe_2S_2(^{Pr}bbimH)(^{Pr}bbim)](Et_4N), 3. **.....S-24**
Figure S16. pK_a determination of **3**.....**S-26**
pK_a Determination of [Fe_2S_2(^{Pr}bbimH)(^{Pr}bbim)](Et_4N)$_2$, 4. **.....S-26**
Figure S17. pK_a determination of **4**.....**S-27**
Electrochemistry**.....S-28**
Figure S18. CVs of **1** (1 mM in 0.25 [^{n}Bu$_4$]PF_6, MeCN) obtained at different scan-rates. **.....S-29**
Figure S19. Scan-rate dependence of current for the CV of **1.** **.....S-30**
Figure S20. CV of **4** and proposed ladder scheme**.....S-31**
Figure S21. Comparison of the CV of **2** and **4**.....**S-32**
Double Mixing Stopped-Flow Kinetics **.....S-33**
Figure S22. Exemplary stopped-flow data of the reaction between **4** and excess TEMPO **.....S-34**
Figure S23. *Pseudo* first order plots of the reaction between **4** and excess TEMPO**. S-35**
Figure S24. Eyring plot for the reaction of **4** with TEMPO.. **.....S-36**
***NMR monitoring of the decomposition of* 3. .....S-37**
***NMR monitoring of the decomposition of* 4. .....S-37**
Figure S25. Stacked ^{1}H NMR spectra (MeCN-d_3) of the decomposition product of **4** **.....S-38**
Table S1: Reduction potentials for various quinones in MeCN. **.....S-39**

General Considerations

Unless noted, all manipulations were carried out using standard Schlenk or glove-box techniques under a dinitrogen atmosphere. Glassware was oven-dried for 24 h prior to use. Celite and molecular sieves were dried by heating to 300 ^{o}C under vacuum for 24 h. Unless otherwise noted, solvents were deoxygenated and dried by sparging with Ar followed by passage through Grubbs-style columns filled with activated alumina.[1] Tetrahydrofuran was further dried by stirring over sodium/benzophenone and vac-transferring. Acetonitrile was purchased from Burdick and Jackson® (< 5ppm low-water brand) and stored in an Ar pressurized stainless steel drum plumbed directly into a glove-box. Dimethylformamide was degassed and dried over activated 3 Å molecular sieves. Nonhalogenated solvents were tested with a standard purple solution of benzophenone ketyl in THF to confirm effective oxygen and moisture removal, and all glove-box solvents were stored over activated 3 Å molecular sieves. Deuterated solvents were purchased from Cambridge Isotopes Laboratories, Inc. and were degassed and stored over activated 3 Å molecular sieves prior to use. d_3-MeCN was dried over CaH_2 and vac-transferred prior to storage over sieves.

Spectroscopic Measurements

NMR spectra were collected on Bruker 300 or 500 MHz spectrometers, and ^{1}H chemical shifts were referenced to residual solvent. MestReNova (6.2.1) was used for NMR data workup. Solution magnetic moments were measured using Evans method.[2] For these measurements, the room temperature densities of DMF and d_7-DMF were employed.

EPR spectra were collected on a Bruker EMX CW X-band spectrometer outfitted with a cryo-cooled cavity. Spectra were collected in a 2:3 MeCN:toluene glass at 120 K at 9.316 GHz (the attenuator was 20.0 dB). The static field was 2800.0 G. The receiver gain was set to 4.48 x 10^4 with a modulation amplitude of 10 G (the modulation frequency was set to 100 kHz). The time constant and conversion time were set to 20.48 ms and 81.92 ms, respectively. EPR spectra were simulated using the W95EPR program.[3] Unless noted, the derivative curves were fit to a Gaussian.

IR measurements were obtained with an NaCl solution cell or a KBr pellet using a Bruker Tensor 27 spectrometer controlled by Opus (version 5.5) software. Typical data were collected between 800 – 4000 cm^{-1} with a resolution of 1 cm^{-1}, and the final spectra were averages of 8 – 100 scans. KBr was dried under vacuum for 12 h at 120 ^{o}C.

Optical spectroscopy measurements were taken on a Hewlett-Packard 8453 diode array spectrophotometer equipped with a Unisoku sample holder that has a temperature controller and magnetic stirrer. Unless noted, all optical spectroscopy measurements were done in MeCN. Samples were taken using quartz cuvettes sealed to a Teflon valve (Kontes) and 14/20 ground-glass joint. For titrations of **2** with acid and base, samples were loaded into a cuvette with a stir bar and the valve closed. A rubber septum was attached to the ground-glass joint, which was

(1) Pangborn, A. B.; Giardello, M. A.; Grubbs, R. H.; Rosen, R. K.; Timmers, F. J., *Organometallics* **1996**, *15*, 1518.
(2) Schubert, E. M., *J. Chem. Educ.* **1992**, *69*, 62.
(3) Neese, F., *QCPE Bull.* **1995**, *15*, 5.

subsequently punctured by needles attached to gas-tight syringes loaded with reagent. Upon removal from the glove-box, the septum was tightened by copper-wire, and the headspace in the cuvette was purged with a constant stream of Ar for 30 min. Reagents were added to the stirring solution by briefly opening the Teflon valve, injecting the reagent, and immediately closing the valve, to ensure minimal contamination by adventitious oxygen. For titrations of **1** with acid/base, samples were prepared in injectable screw-capped cuvettes with a silicone septum (Starna). Acid or base was added via gas-tight syringe from freshly prepared samples of acid/base stored under a blanket of Ar in septum-capped vials. After each addition, the cuvette was inverted once prior to data collection to ensure proper mixing, and each titration was completed within 5 minutes.

X-ray Crystallography Procedures

Low-temperature diffraction data were collected on a Bruker APEXII single crystal diffractometer coupled to a Bruker APEXII CCD detector with graphite-monochromated Mo Kα radiation (λ = 0.71073 Å), performing φ-and ω-scans. The structures were solved by direct or Patterson methods using SHELXS[4] and refined against F^2 on all data by full-matrix least squares with SHELXL-97.[5] All non-hydrogen atoms were refined anisotropically. All hydrogen atoms were included into the model at geometrically calculated positions and refined using a riding model. The isotropic displacement parameters of all hydrogen atoms were fixed to 1.2 times the U value of the atoms they are linked to (1.5 times for methyl groups). The structures were refined using established methods.[6] Crystals of **1** contained 1 pentane molecule per asymmetric unit, which is disordered over 4 positions about an inversion center. The pentane molecule was refined isotropically, and a free variable was employed to set the U_{iso} equal within the 4 components of the disorder. Additionally, the SAME restraint was employed to render the pentanes equivalent. Crystals of **2** invariably suffered from disorder. Both $(^{Pr}bbim)^{2-}$ ligands in the asymmetric unit contained one disordered propyl group. Additionally, the solvent/Et_4N^+ were highly disordered. Refinement of the individual populations of the Et_4N^+ gave a population of *ca*. 3 Et_4N^+ per iron dimer. Some of the Et_4N^+ sites were also occupied by disordered solvent molecules, and it is conceivable that the additional Et_4N^+ and/or solvent sites are present in the crystal, but the overall quality of the data set precluded our ability to locate these sites. From this a final model was constructed, whereby the populations of the individual components of the disorder were not allowed to vary, was employed.

(4) Sheldrick, G. M., *Acta Cryst.* **1990**, *A46*, 467.
(5) Sheldrick, G. M., *Acta Cryst.* **2008**, *A64*.
(6) Müller, P.; Herbst-Irmer, R.; Spek, A. L.; Schneider, T. R.; Sawaya, M. R., *Crystal Structure Refinement: A Crystallographer's Guide to SHELXL*. Oxford University Press: Oxford, 2006.

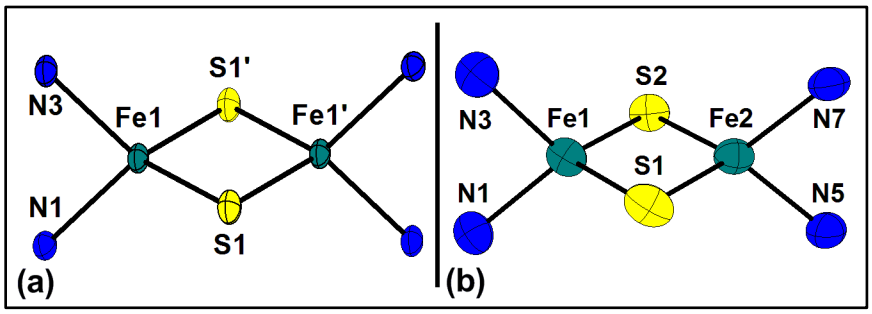

Figure S1. Thermal ellipsoid (50%) representation of the core atoms of (a) di-ferric **1** and (b) mixed-valence **2**. Select bond distances (Å) for 1: Fe1-N1 1.976(2), Fe1-N3 1.980(2), Fe1-S1 2.1914(8), Fe1-S1' 2.2032(8), Fe1-Fe1 2.7063(8). Select bond distances (Å) for **2**: Fe1-N1 2.035(3), Fe1-N3 2.037(3), Fe1-S1 2.212(1), Fe1-S2 2.213(1), Fe2-N5 2.047(3), Fe2-N7 2.073(3), Fe2-S1 2.242(1), Fe2-S2 2.230(1), Fe1-Fe2 2.7123(9).

Starting Materials and Reagents

Reagents were purchased from commercial vendors (Thallium ethoxide was purchased from Strem chemicals; the quinones were purchased from TCI or Fischer Scientific; all other reagents were purchased from Aldrich) and unless noted, used without further purification. 4-Dimethylaminopyridine (DMAP) was crystallized from toluene,[7] triazabicyclodecene (TBD) was crystallized from THF, quinuclidine was crystallized from Et_2O/THF, and 2,5-di-*tert*-butyl-1,4-benzoquinone (2,5^{t}Bu$_2$-Q) was crystallized from acetonitrile. TEMPO (2,2,6,6-tetramethyl-piperidin-1-yl-oxyl) was sublimed under vacuum[7] and $[Et_4N]Cl$ was dried under vacuum for 24 h (50 ^{o}C). [^{n}Bu$_4$N]PF_6 was triply crystallized from EtOH/MeCN and subsequently dried under vacuum for 48 h at 50 ^{o}C. Hexamethyldisiloxane (HMDS) was dried with Na and vac-transferred.

Dipropylmalononitrile,[8] 4,4-bis(benzimidazol-2-yl)heptane (^{Pr}bbimH$_2$),[9] and $[Fe_2S_2Cl_4](Et_4N)_2$[10] were prepared according to literature methods. The 2,5-di-*tert*-butyl-1,4-benzosemiquinone radical anion ([2,5^{t}Bu$_2$-SQ]Na(15-crown-5)) was prepared by modification of literature methods.[11] [DMAP-H]OTf, quinuclidinium triflate, and [pyH]OTf were prepared by addition of 1 equiv triflic acid to the corresponding base in Et_2O. The resulting precipitates were isolated, and recrystallized from MeCN. [DMAP-D]OTf was prepared analogously using DOTf. [DBU-H]OTf (DBU = 1,8-diazabicycloundec-7-ene) was prepared by addition of 1 equiv triflic acid to the corresponding base in Et_2O. After stirring for 30 min, the volatiles were removed and the resulting oil dried under vacuum for 24 h. $[Fe_2S_2(^{Pr}bbim)_2](Et_4N)_2$ (**1**) and $[Fe_2S_2(^{Pr}bbim)_2](Et_4N)_3$ (**2**) were prepared by modification of literature methods;[9] their syntheses and additional characterizations are described below.

Synthesis of Clusters

Synthesis of ^{Pr}bbimTl$_2$. Thallium ethoxide (98 %, 0.6098 g, 2.4 mmol), in 2 mL MeCN was added to a stirring suspension of ^{Pr}bbimH$_2$ (0.3620 g, 1.089 mmol) in 8 mL MeCN. After stirring for 1 h, the reaction was concentrated to 2 mL and filtered. The solids were isolated on a frit, rinsed with 3 x 10 mL pentane, and dried (0.6674 g, 83 %). ^{1}H NMR (DMSO-d_6, 300 MHz, 25 ^{o}C): δ 7.42 (bs, Ar*H*, 4H), 6.75 (bs, Ar*H*, 4H), 2.39 (bs, CH_2, 4H), 1.13 (bs, CH_2, 4H), 0.83 (bs, CH_2, 6H).

Synthesis of $[Fe_2S_2(^{Pr}bbim)_2](Et_4N)_2$, 1. As noted above, **1** was prepared by modification of Gibson's procedure. A suspension of ^{Pr}bbimTl$_2$ (0.6674 g, 0.9030 mmol) in 10 mL MeCN was added drop-wise over 5 min to a stirring solution of $[Fe_2S_2Cl_4](Et_4N)_2$ in 10 mL of MeCN. The reaction stirred for 90 min, at which time the volatiles were removed. The dark purple solids were extracted into 50 mL THF, then into 10 mL MeCN, and both solutions were filtered through a Celite-lined frit. The MeCN fraction was layered with Et_2O to obtain crystals of **1**

(7) Armarego, W. L. F.; Chai, C. L. L., *Purification of Laboratory Chemicals*. 5 ed.; Butterworth-Heinmann: London, 2002.
(8) Bloomfield, J., *J. Org. Chem.* **1961**, *26*, 4112.
(9) Beardwood, P.; Gibson, J. F., *J. Chem. Soc., Dalton Trans.* **1992**, 2457.
(10) Do, Y.; Simhon, E. D.; Holm, R. H., *Inorg. Chem.* **1983**, *22*, 3809.
(11) Lü, J.-M.; Rosokha, S. V.; Neretin, I. S.; Kochi, J. K., *J. Am. Chem. Soc.* **2006**, *128*, 16708.

(0.0617 mg, 12.5 %). The THF fraction was concentrated to dryness, the resulting solids dissolved in 10 mL MeCN, and crystals of **1** were obtained upon storage at - 35 ^{o}C for 24 h (0.2311 g, 47%). Crystals suitable for XRD were grown from the vapor diffusion of pentane into a saturated solution of **1** in THF. ^{1}H NMR (MeCN-d_3, 500 MHz, 25 ^{o}C): δ 10.71 (s, Ar-H, 4H), 7.03 (s, Ar-H, 4H), 6.3 (bs, Ar-H), 5.61 (s, Ar-H, 4H), 3.29 (bs, CH_2, 8H), 3.05 (bs, N$CH_2$$CH_3$, 16H), 1.73 (s, CH_2, 8H, overlapping with solvent), 1.13 (bs, NCH$_2$$CH_3$, 24H), 0.93 (s, CH_3, 12H). Similar chemical shifts are observed in DMF-d_7 (500 MHz, 25 ^{o}C): δ 10.70 (s, Ar-H, 4H), 7.02 (s, Ar-H, 4H), 6.6 (bs, Ar-H), 5.58 (s, Ar-H, 4H), 3.34 (bs, overlapping NCH_2CH$_3$ and CH_2, 24H), 1.88 (bs, CH_2, 8H), 1.26 (bs, NCH$_2$$CH_3$, 24H), 0.93 (s, CH_3, 12H). COSY (DMF-d_7) was used to aid in peak assignment. UV-vis (MeCN) λ_{max}, nm (ε, M^{-1} cm^{-1}): 408 (7340), 439 (sh, 7150), 478 (sh, 6790), 526 (7880), 670 (sh, 710).

Synthesis of [Fe$_2$S$_2$(^{Pr}bbim)$_2$](Et$_4$N)$_3$, 2. As noted above, **2** was prepared by modification of Gibson's procedure. Solid [Et$_4$N]Cl (0.0160 g, 0.0966 mmol) was added to a stirring solution of **1** (0.1060 g, 0.0966 mmol) in 15 mL THF. To this, 0.424 wt% Na/Hg (0.5450 g, 0.10 mmol) was added, and the reaction stirred for 1 h. The reaction mixture was filtered through a Celite-lined frit, and the maroon solids rinsed with 3 x 2 mL THF. The solids were then extracted into 20 mL MeCN and filtered through a Celite-lined frit, leaving behind pale gray salts. The filtrate was concentrated to *ca*. 6 mL MeCN and layered with Et$_2$O to afford crystals of **2** (0.0738 g, 62 %). A second crop of crystals was obtained by concentrating the mother liquor and layering with Et$_2$O (0.0238 g, 20 %). ^{1}H NMR (MeCN-d_3, 500 MHz, 25 ^{o}C): δ 12.16 (s, Ar-H, 4H), 6.45 (s, Ar-H, 4H), 6.2 (bs, Ar-H, 4H), 5.48 (s, Ar-H, 4H), 3.70 (bs, CCH_2, 8H), 2.65 (s, NCH_2CH$_3$, 24H), 1.94 (s, CCH$_2$$CH_2$, 8H, overlapping with solvent), 0.98 (s, CH_3, 12H), 0.87 (s, NCH$_2$$CH_3$, 36H). COSY (MeCN-$d_3$) was used to aid in peak assignment. UV-vis (MeCN) λ_{max}, nm (ε, M^{-1} cm^{-1}): 387 (sh, 3810), 434 (sh, 1910), 487 (sh, 1610), 532 (2190), 580 (1264), 860 (300). Evans method (DMF-d_7, -25 ^{o}C): 2.3 B.M. X-band EPR (9.32 GHz, 120 K, 2:3 MeCN:toluene): g = [2.012, 1.940, 1.835], W = [40, 70, 145 G].

Generation of [Fe$_2$S$_2$(^{Pr}bbimH)(^{Pr}bbim)](Et$_4$N), 3. A 1.94 mM solution of **1** in d_3-MeCN (1.00 mL, 1.94 μmol) was prepared and transferred to an NMR tube that was capped with a rubber septum and parafilmed. To this, 64 μL of a 30 mM solution of [pyH]OTf in d_3-MeCN (1.9 μmol) was added via gas-tight syringe. The NMR tube was immediately inverted 3 times to ensure full mixing. Cluster **3** can be prepared analogously in the glove-box by addition of acid ([pyH]OTf or [DMAP-H]OTf) to a stirring solution of **1**. Cluster **3** is not thermally stable, decomposing over hours (at room temperature) to several species. ^{1}H NMR (MeCN-d_3, 500 MHz, 25 ^{o}C): δ 10.65 (s, Ar-H, 4H), 7.05 (s, Ar-H, 4H), 6.4 (bs, Ar-H), 5.73 (s, Ar-H, 4H), 3.26 (bs, CH_2, 8H), 3.09 (s, NCH_2CH$_3$, 16H), 1.74 (s, CH_2, 8H, overlapping with solvent), 1.16 (s, NCH$_2$$CH_3$, 24H), 0.95 (s, CH_3, 12H). UV-vis (MeCN) λ_{max}, nm (ε, M^{-1} cm^{-1}): 382 (sh, 5560), 410 (5730), 488 (sh, 5620), 526 (6310), 655 (sh, 900).

Synthesis of [Fe$_2$S$_2$(^{Pr}bbimH)(^{Pr}bbim)](Et$_4$N)$_2$, 4. A 5.70 mM solution of **2** in d_3-MeCN (600 μL, 3.42 μmol) was prepared and transferred to an NMR tube that was capped with a rubber septum and parafilmed. The sample was frozen with lN$_2$, and 50 μL of a 68 mM solution of [DMAP-H]OTf in d_3-MeCN (3.4 μmol) was added via gas-tight syringe. The sample was thawed and inverted 3 times to ensure full mixing. Cluster **4** can be prepared analogously in the glove-box by addition of acid ([pyH]OTf or [DMAP-H]OTf) to a stirring solution of **2** in MeCN (at -20

^{o}C). Cluster **4** is not thermally stable, decomposing over minutes (at room temperature) to several species. ^{1}H NMR (MeCN-d_3, 500 MHz, –20 ^{o}C): **δ** 120 (bs), 19.7 (bs), -2 – 10 (bs), 2.91 (Et_4N^+), 0.83 (Et_4N^+). Cluster **4** is essentially NMR silent at all temperatures monitored in both MeCN-d_3 (-20 to 25 ^{o}C) and DMF-d_7 (-50 to 25 ^{o}C) between ±170 ppm (500 MHz). UV-vis (MeCN, –20 ^{o}C) λ_{max}, nm (ε, M^{-1} cm^{-1}): 527 (2500), 578 (1600), 642 (sh, 760), 737 (470), 852 (360). Evans method (DMF-d_7, –25 ^{o}C): 2.4 B.M. X-band EPR (9.32 GHz, 120 K, 2:3 MeCN:toluene): g = [1.983, 1.943, 1.860], W = [61, 22, 84 G]. The EPR of **4**-D (prepared by reacting **2** with [DMAP-D]OTf was indistinguishable from that of **4**.

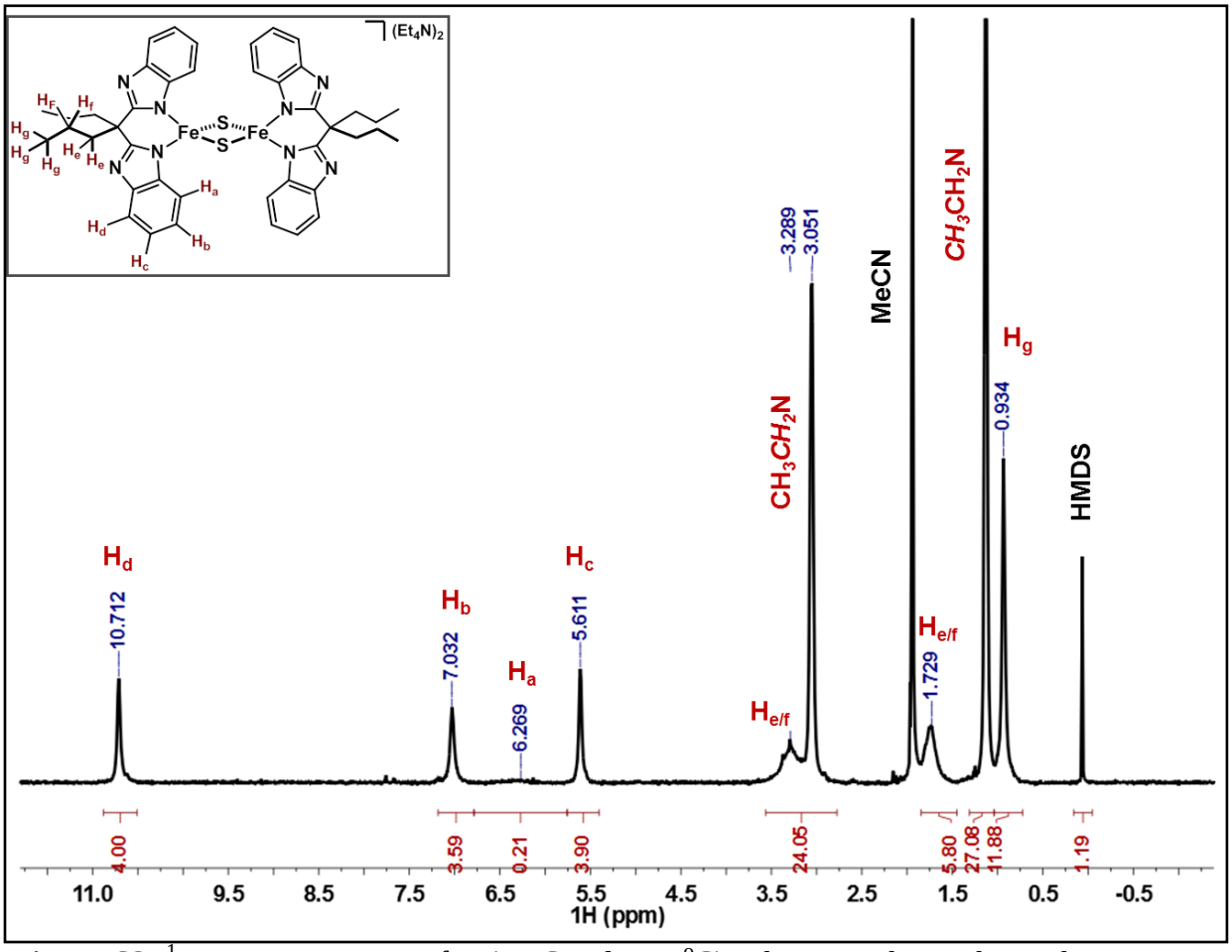

Figure S2. ^{1}H NMR spectrum of **1** (MeCN-d_3, 25 ^{o}C). The inset shows the peak assignments. The broadness of the resonance at 6.3 ppm suggests that it is close to the metal centers, and hence is assigned as the H_a resonance. The resonances at 10.71, 7.03, and 5.61 are assigned as the other Ar-H resonances based on their integration values and the observance of correlations between them (see Figure S3). The distinction between H_d and H_b was made on the assumption that a spin polarization mechanism dominates the hyperfine shifting of the resonances.[12]

(12) Que, J., Lawrence, *Physical Methods in Bioinorganic Chemistry* University Science Books: Sausalito, CA, 2000.

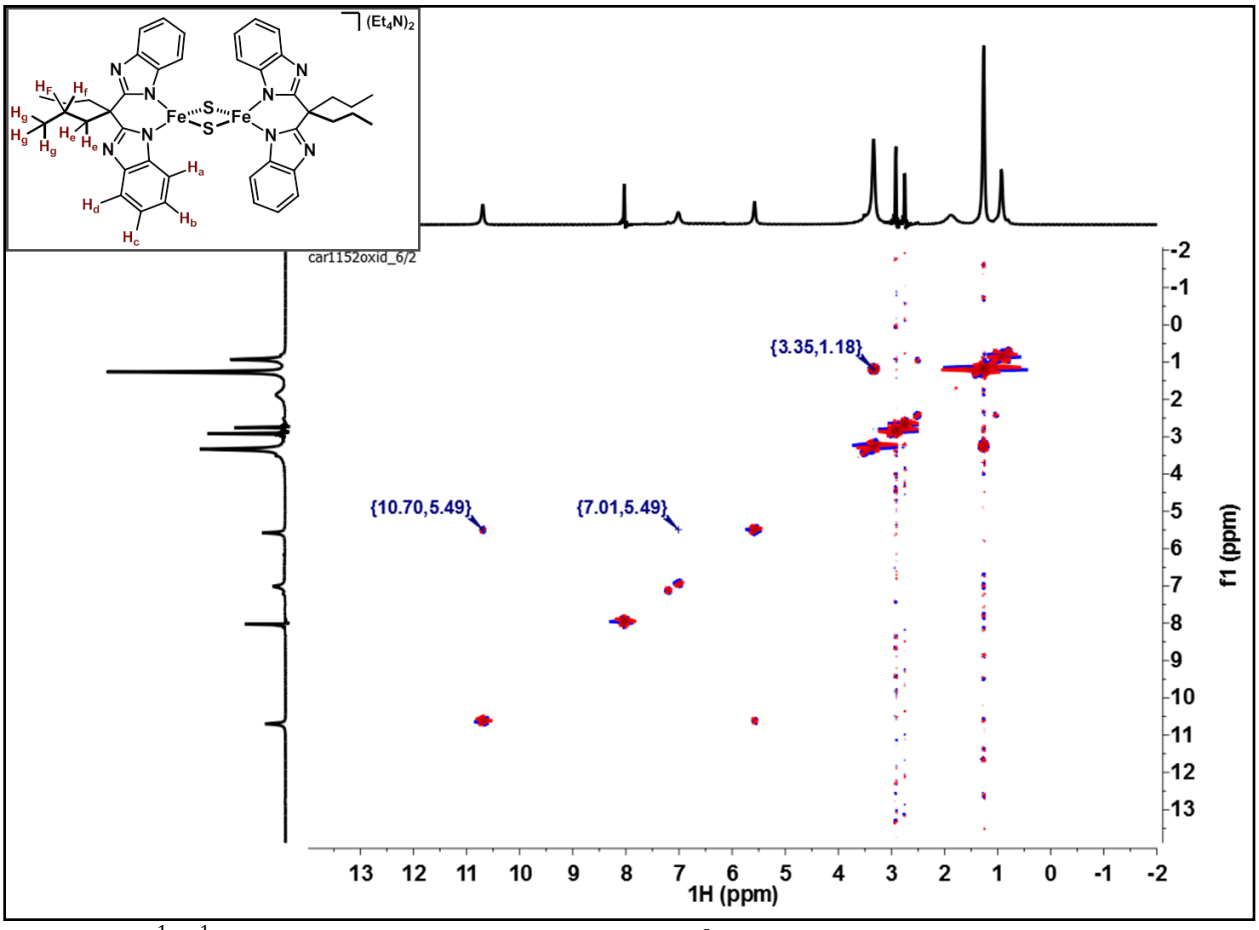

Figure S3. $^{1}H/^{1}H$ COSY spectrum of **1** (DMF-d_7, 25 ^{o}C). The inset shows the peak assignments (see Figure S2).

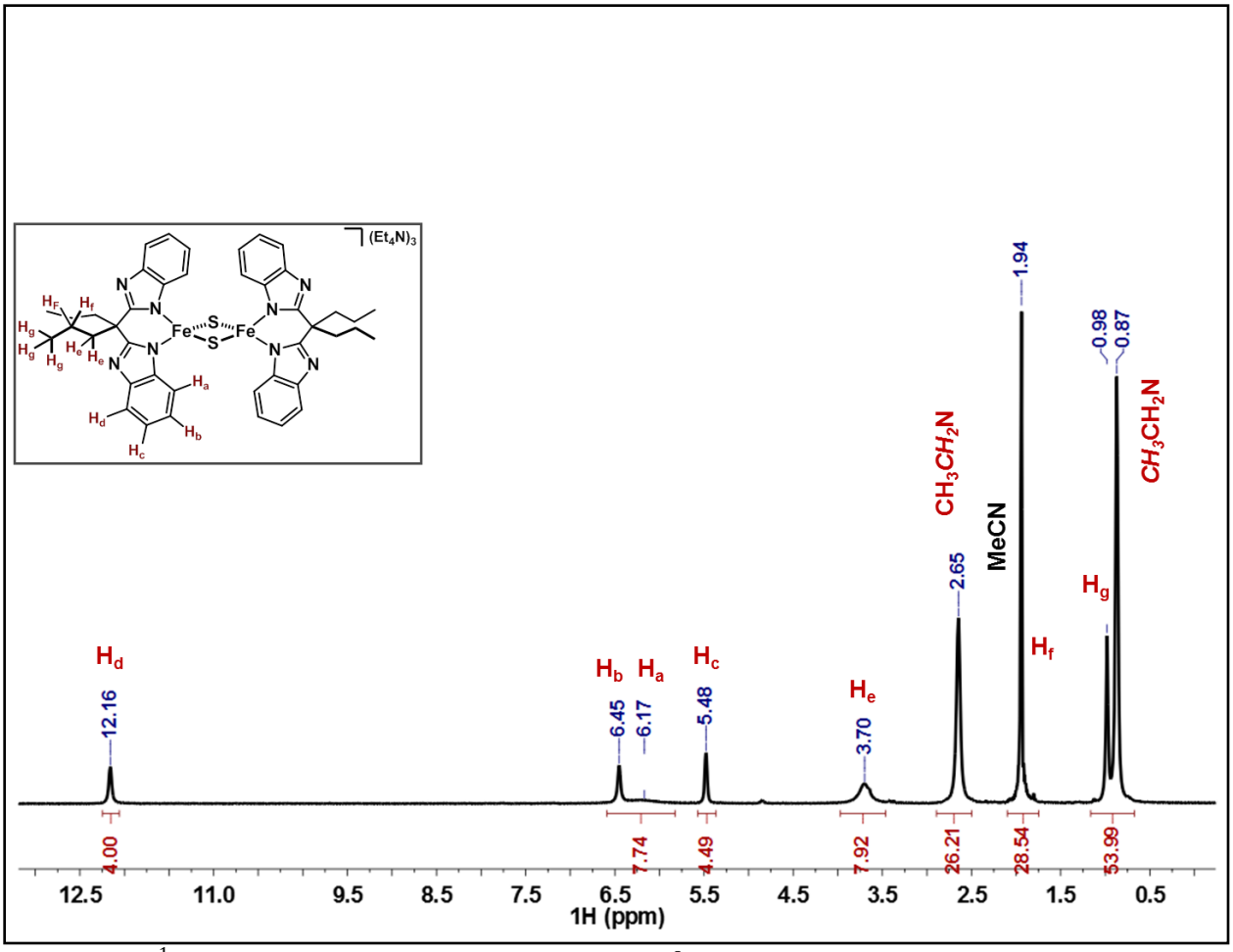

Figure S4. ^{1}H NMR spectrum of **2** (MeCN-d_3, 25 ^{o}C). The inset shows the peak assignments (see Figure S2 caption and Figure S5).

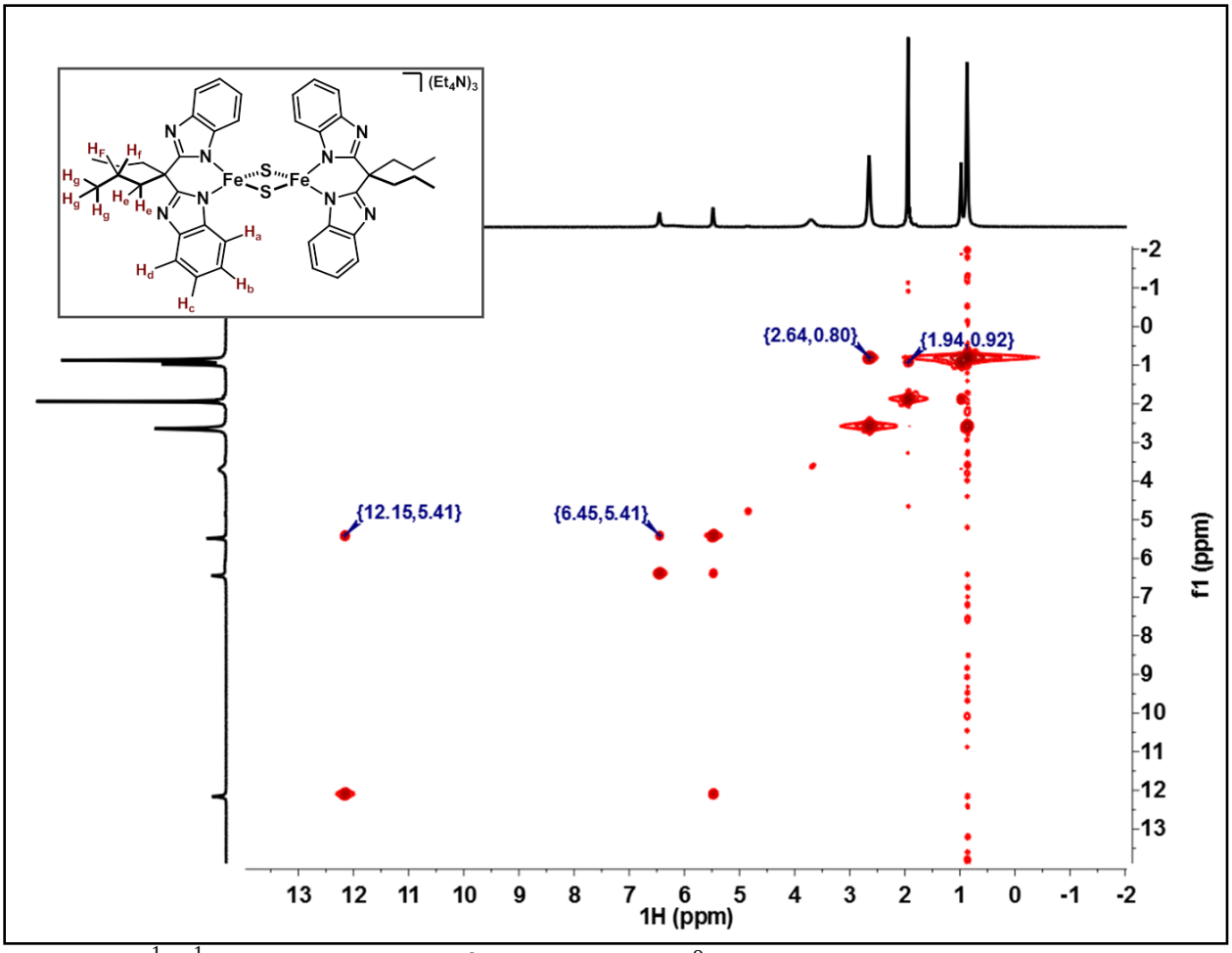

Figure S5. $^{1}H/^{1}H$ COSY spectrum of **2** (MeCN-d_3, 25 ^{o}C). The inset shows the peak assignments (See Figure S4).

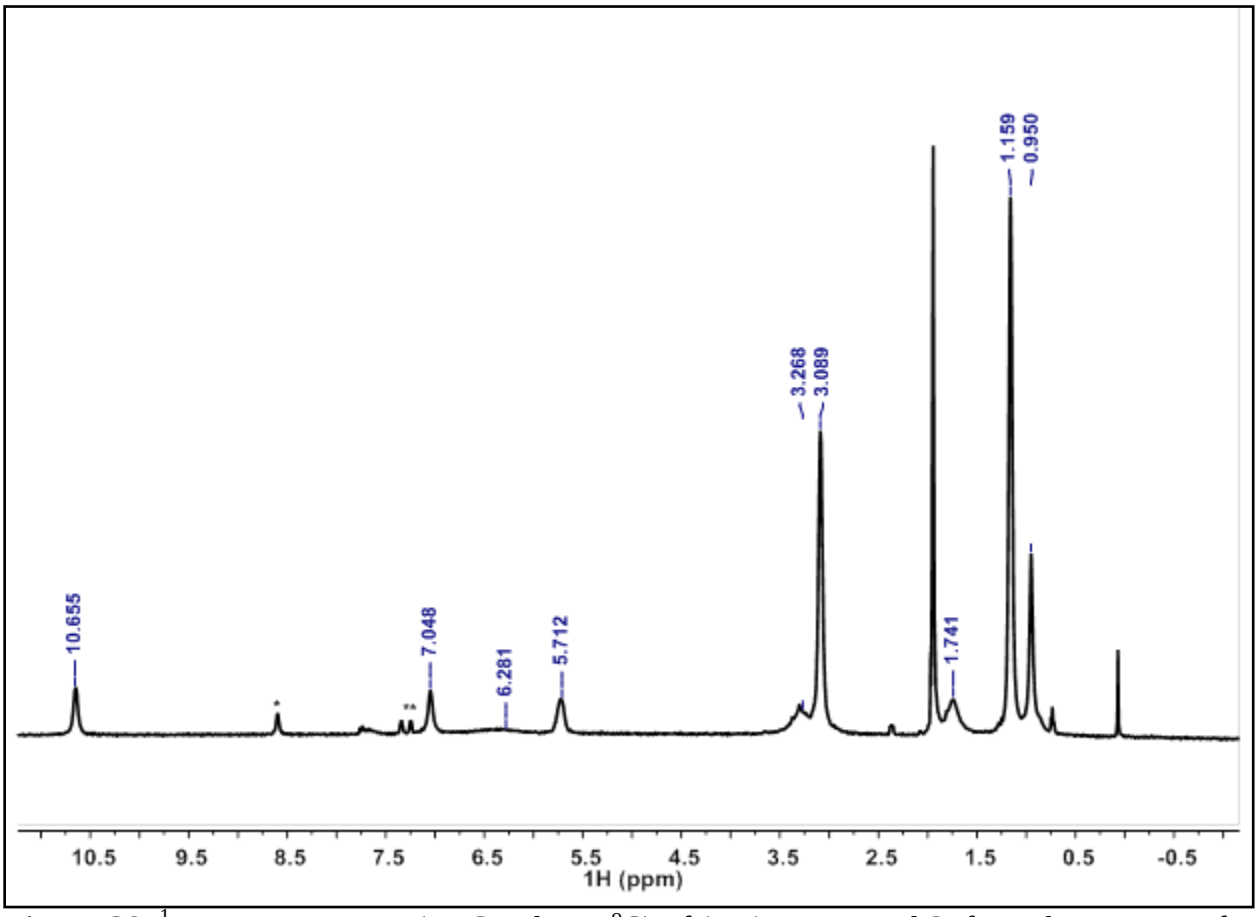

Figure S6. ^{1}H NMR spectrum (MeCN-d_3, 25 ^{o}C) of *in situ* generated **3**, from the reaction of **1** with [pyH]OTf. Peaks from the resulting pyridine are marked (*).

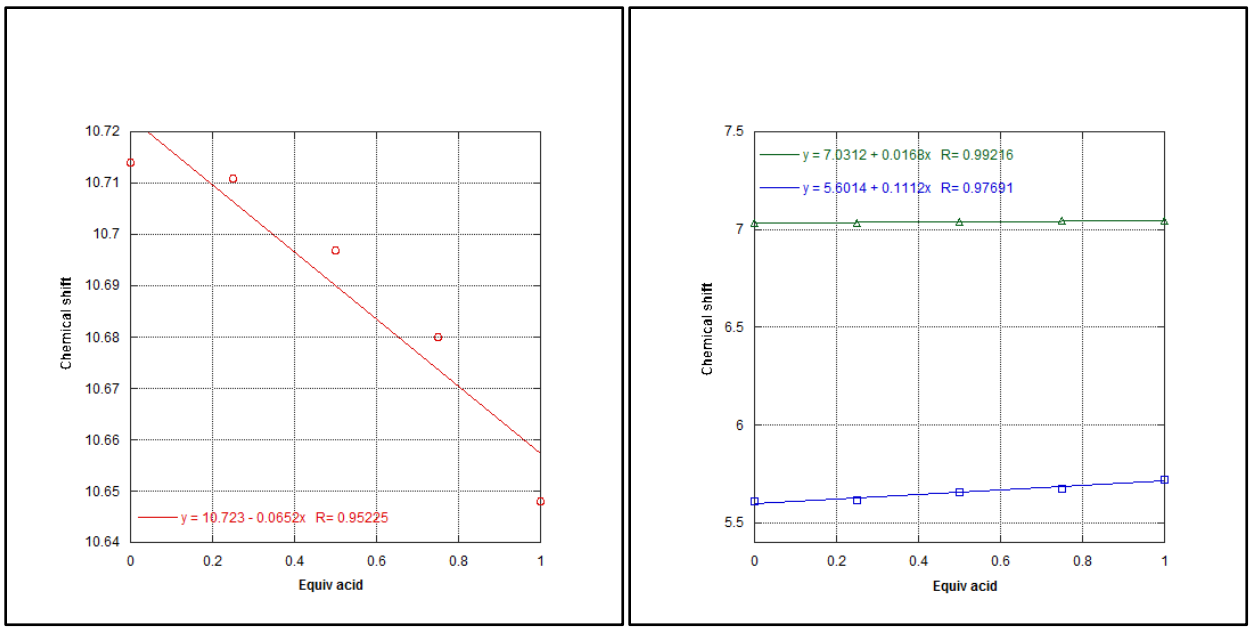

Figure S7. Plots of chemical shift (Ar-H) *vs.* equiv acid ([pyH]OTf) added to **1** (MeCN-d_3, 25 ^{o}C). Proton transfer between **1** and **3** is rapid on the NMR timescale.

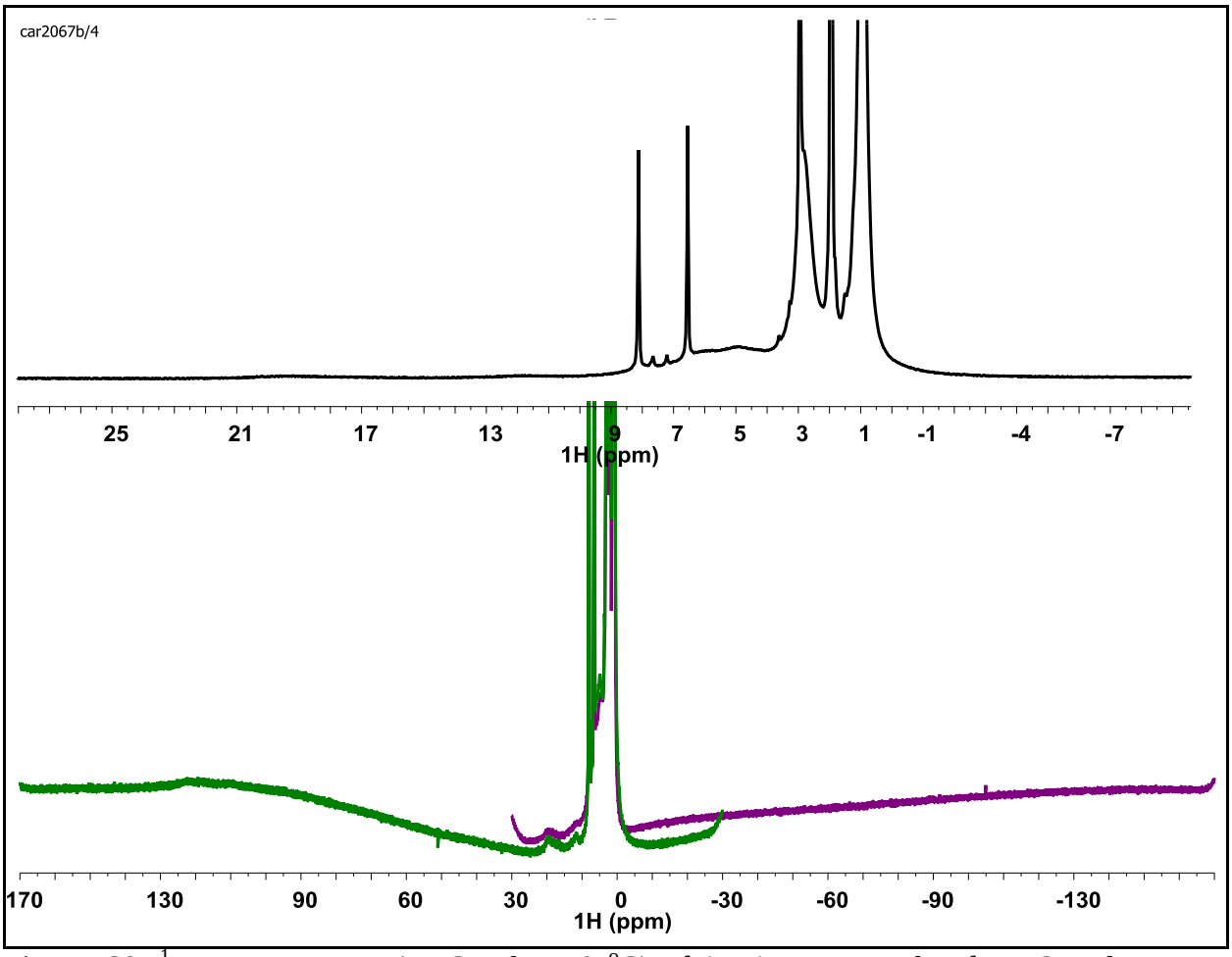

Figure S8. ^{1}H NMR spectra (MeCN-d_3, –20 ^{o}C) of *in situ* generated **4** from **2** and 1 equiv [DMAP-H]OTf. (top): Spectrum shown between -10 and 28 ppm, indicating the broad feature between 0 and 9 ppm (the baseline is not flat). The peaks at 8.1 and 6.5 ppm are due to DMAP. (bottom): Superposition of spectra showing a chemical shift window of ± 170 ppm.

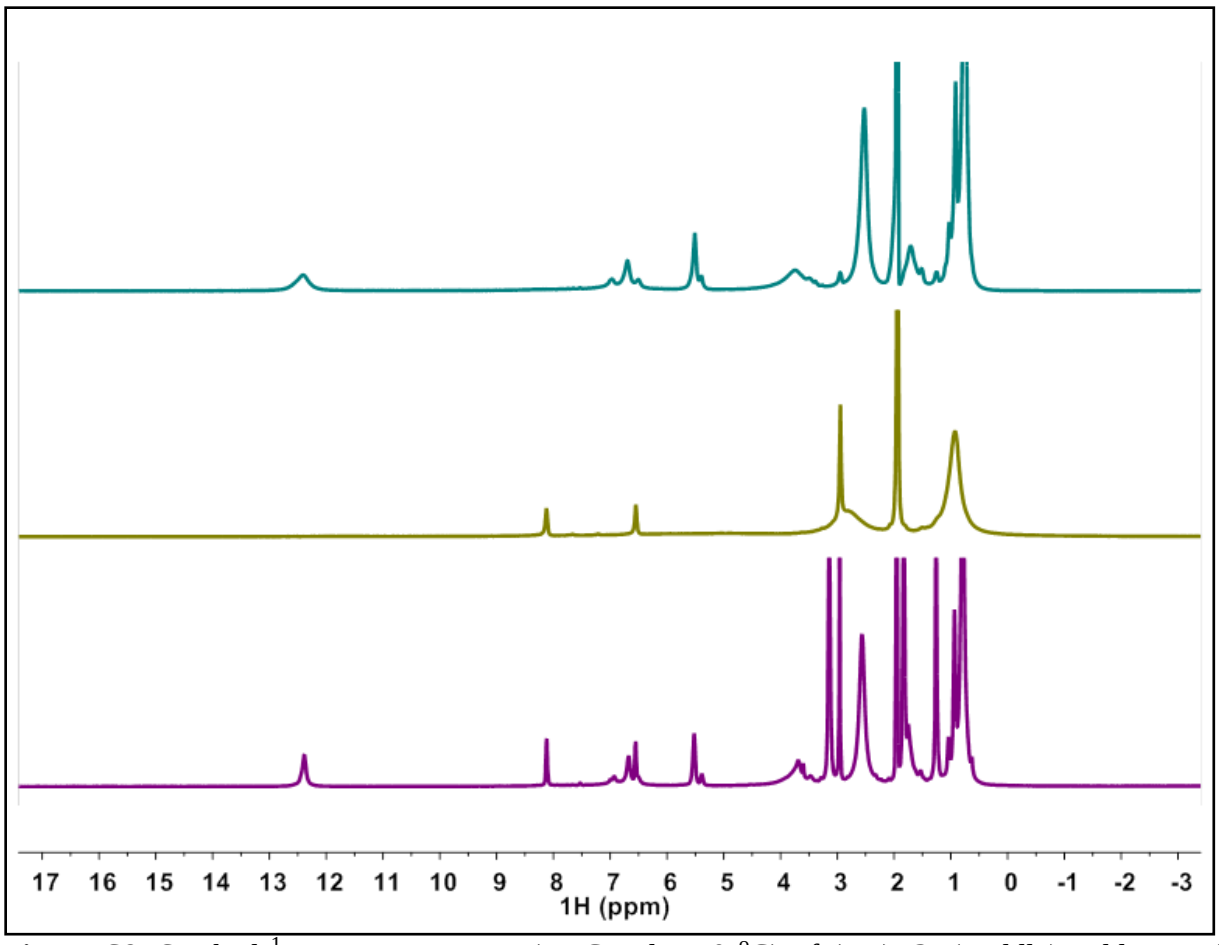

Figure S9. Stacked ^{1}H NMR spectrum (MeCN-d_3, -20 ^{o}C) of (top): **2**; (middle): addition of 1 equiv [DMAP-H]OTf to generate **4**; (bottom): addition of 1 equiv of ^{t}BuN=P(pyrr)$_3$ to regenerate **2**.

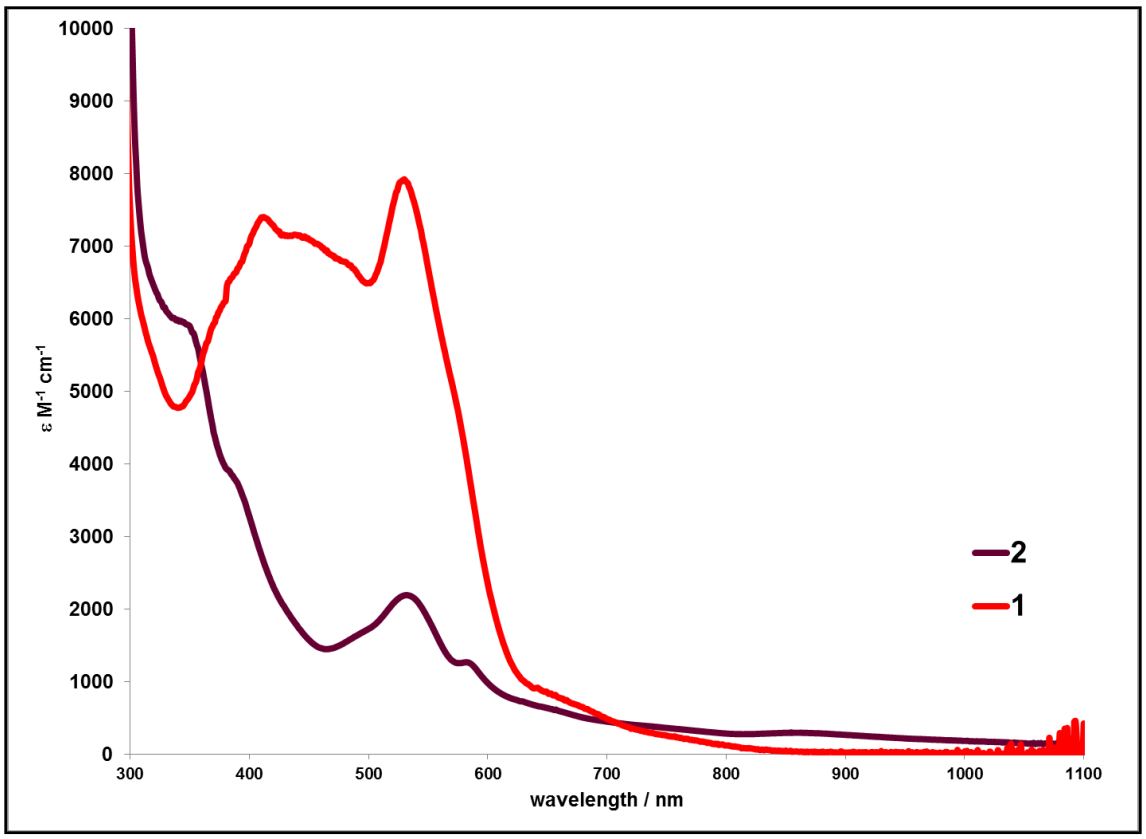

Figure S10. UV-vis spectra of **1** and **2** in MeCN.

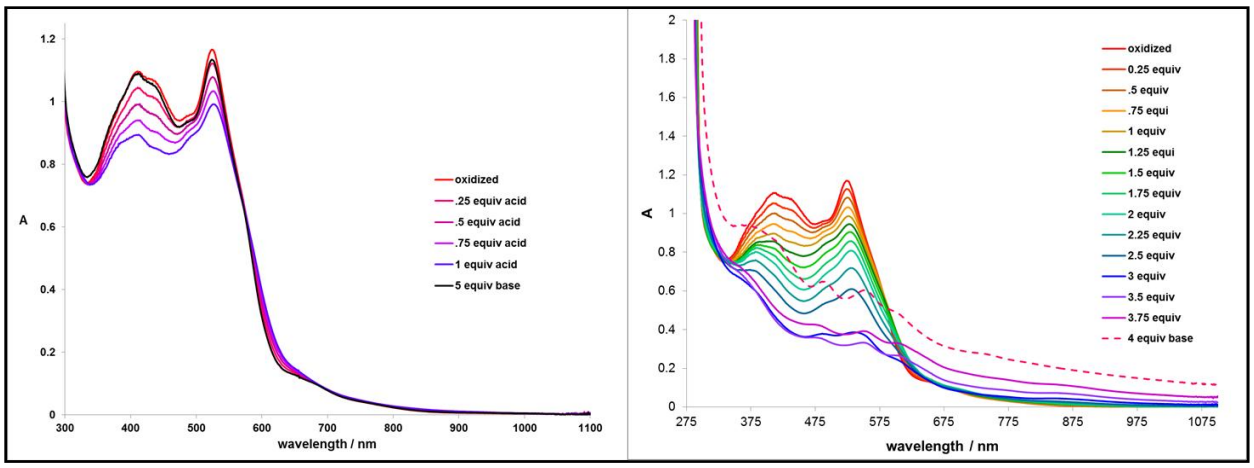

Figure S11. Stacked UV-vis spectra (MeCN) of **1** in the presence of acid ([pyH]OTf) and then base (DBU). (left): In the presence of ≤ 1 equiv acid, **1** is reversibly protonated to **3**. Isosbestic points at 332and 579 nm are observed. (right): Upon addition of > 1 equiv acid, the protonation(s) of **1** become irreversible; the isosbestic points are lost, and addition of base (DBU) does not regenerate **1**.

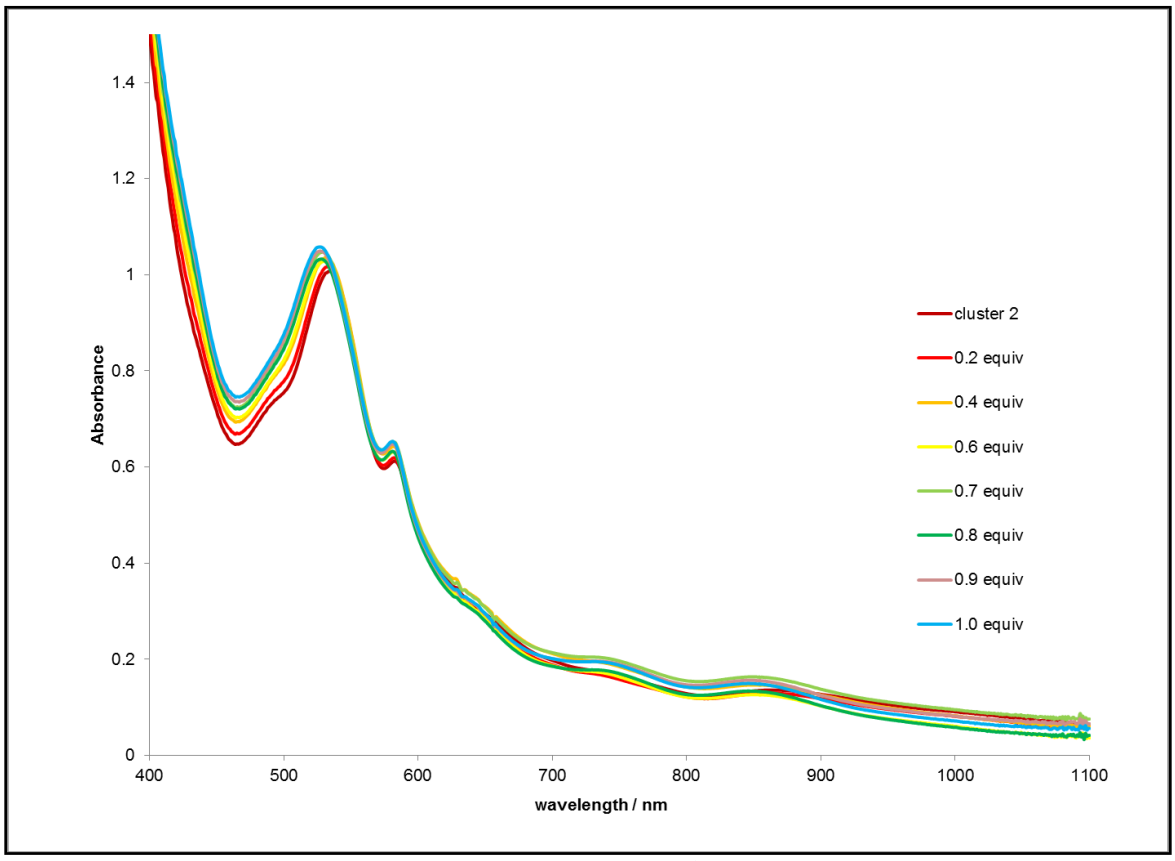

Figure S12. Stacked UV-vis spectra (MeCN, –20 ^{o}C) of **2** with increasing amounts of acid ([DMAP-H]OTf), showing a small shift in the peak at 532 nm (**2**) to 527 (**4**) nm.

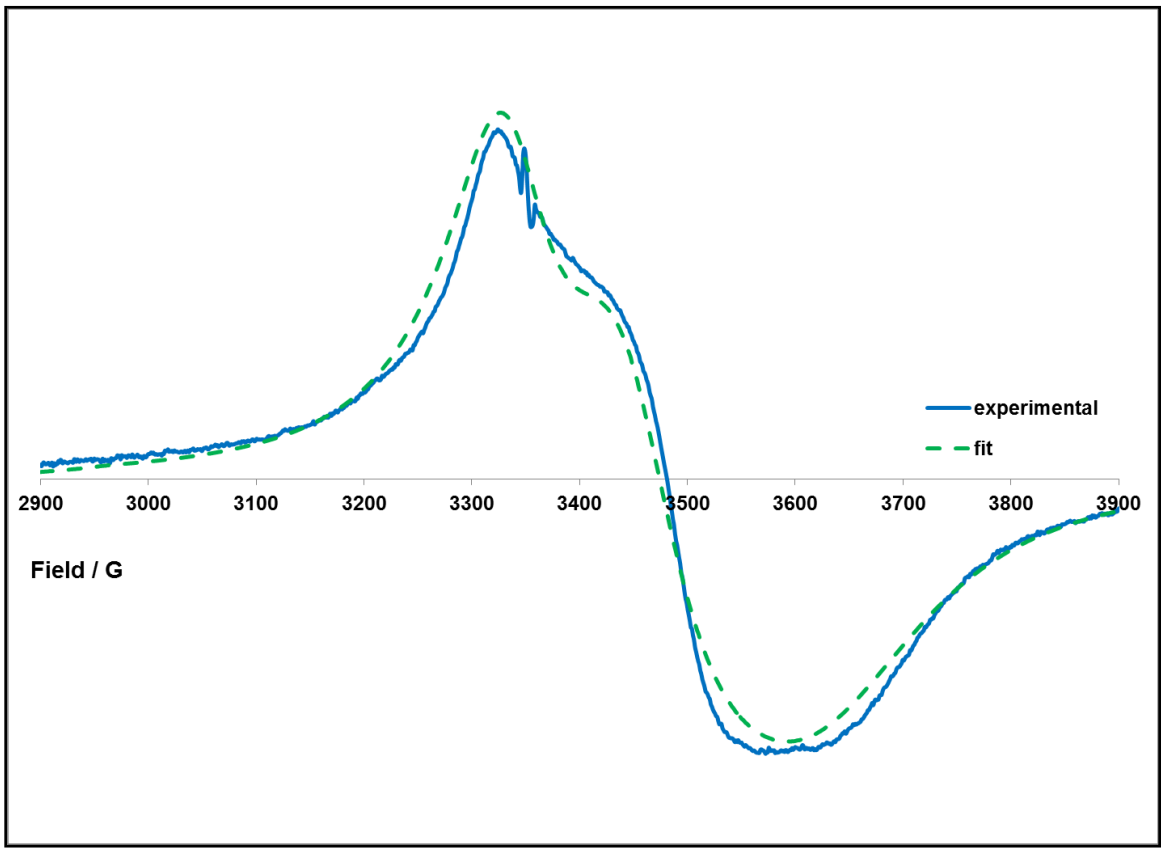

Figure S13. EPR spectrum of **2** obtained at 120 K in a 2:3 MeCN:toluene glass. The spectrum was fit using Lorentzian lineshape to give g = [2.012, 1.940, 1.835] and W = [40, 70, 145 G]. The sharp peak at ca. 3360 G is due to an impurity.

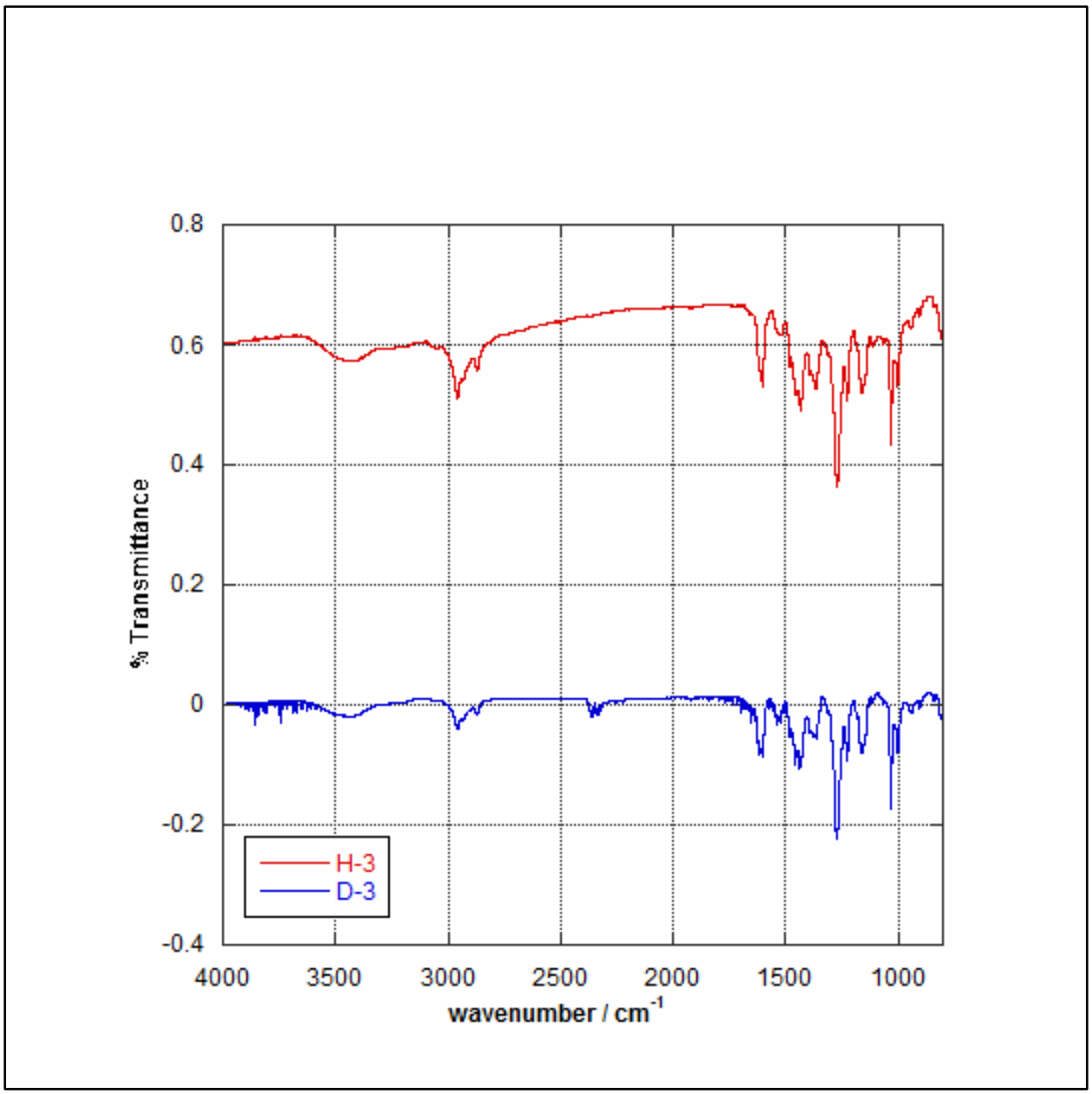

Figure S14. Stacked IR spectra (KBr) of **H-3** (red, top) and **D-3** (blue, bottom). No obvious N-H(D) or S-H(D) stretches could be observed. Similar spectra were obtained in solution (MeCN or DMF). Samples were prepared by addition of MeCN solutions of [DMAP-H]OTf and [DMAP-D]OTf to an MeCN solution of **1**. After stirring for 5 min, the volatiles were removed and KBr pellets prepared.

Reaction of 4 with oxidants.

In a typical experiment, a solution of **2** (4.5 mM) in d_3-MeCN was prepared, and HMDS (1.1 mM) was added as an internal standard (hexamethylbenzene was alternatively used as an internal standard; HMDS = hexamethyldisiloxane = $Me_3SiOSiMe_3$). Solutions of acid ([pyH]OTf or [DMAPH]OTf) and oxidant (TEMPO, 2,5^{t}Bu$_2$-Q, duraquinone, 2-methyl-5,6-di-methoxy-*p*-benzoquinone, or [2,5^{t}Bu$_2$-SQ]Na(15-crown-5)) were prepared in d_3-MeCN (*ca.* 54.0 mM). The solution of **2** (typically 0.5 – 0.7 mL) was transferred to vials containing stir bars. To a stirring solution of **2**, 1 equiv of acid (typically 25 – 50 μL) was added. After stirring for 15 seconds, the oxidant (1 equiv for TEMPO and [2,5^{t}Bu$_2$-SQ]Na(15-crown-5), 0.5 equiv for Q) was added, during which the solution changed color from maroon to bright red. The solution was transferred to an NMR tube, and the ^{1}H NMR spectrum recorded within 30 min of the start of the reaction.

Alternatively, solutions of **2** were transferred to NMR tubes that were capped with a rubber septum and parafilmed. The ^{1}H NMR spectrum of **2** was obtained. Via gas-tight syringe, 1 equiv of acid was added, the tube inverted twice, then oxidant (1 equiv for TEMPO and [2,5^{t}Bu$_2$-SQ]Na(15-crown-5), 0.5 equiv for the quinone oxidants), was added. The tube was inverted twice, and the ^{1}H NMR spectrum of the reaction was recorded.

Control experiments, in which **2** was treated first with oxidant then with acid, were done as described above, with the exception that a ^{1}H NMR spectrum was recorded between additions of oxidant and acid.

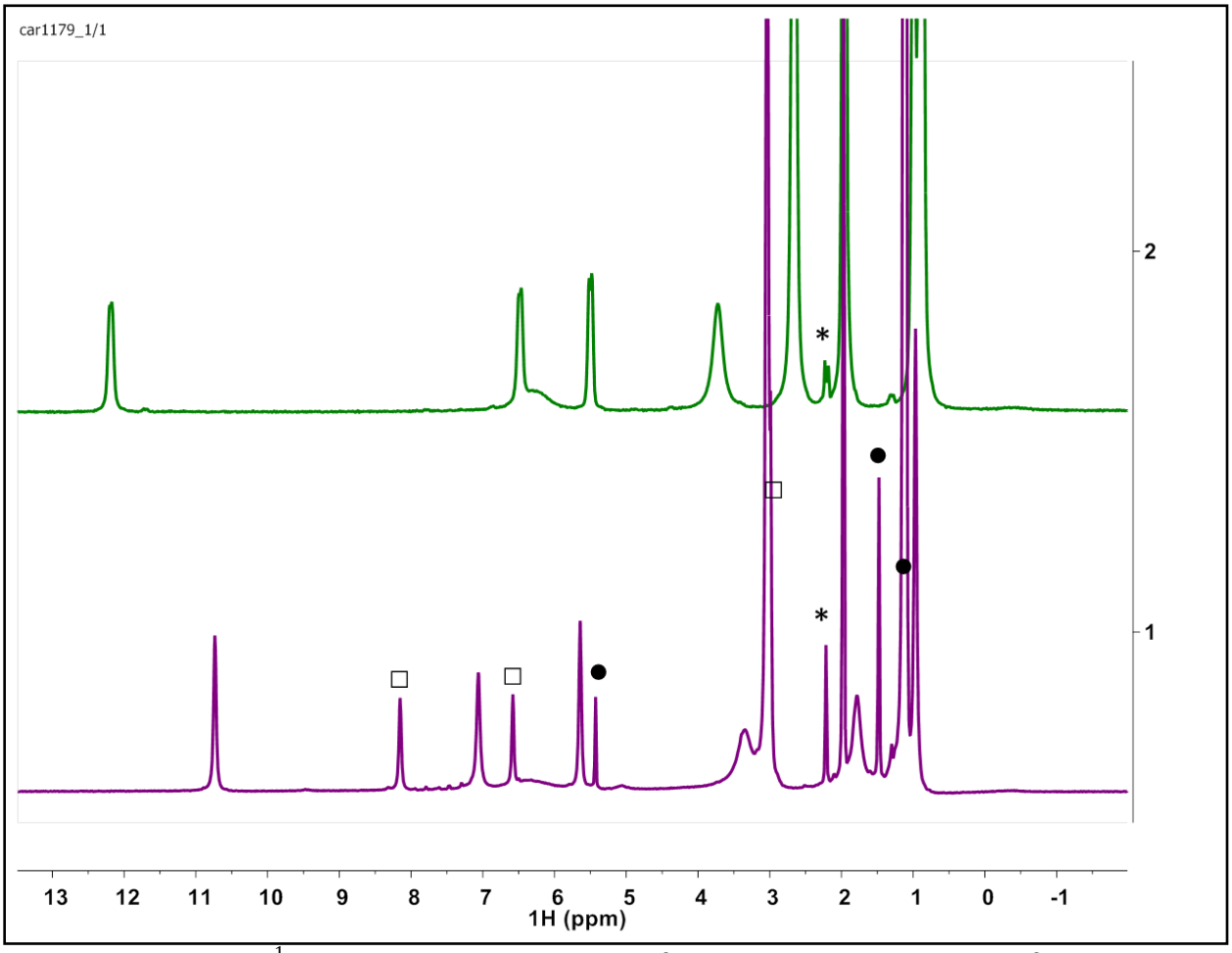

Figure S15. Stacked ^{1}H NMR spectra (MeCN-d_3) of: (top) **2**; (bottom) reaction of **2** with 1 equiv [DMAP-H]OTf and TEMPO. Peaks marked with black circles correspond to TEMPO-H, black squares correspond to DMAP, and the asterisk corresponds to hexamethylbenzene (internal standard).

pK_a Determination of [Fe_2S_2(^{Pr}bbimH)(^{Pr}bbim)](Et_4N), 3.

Titrations to obtain the pK_a of **3** were monitored by UV-vis spectroscopy. Since **3** can be further protonated which leads to decomposition, the pK_a of **3** was determined by titration of *in situ* generated **3** with a suitable base to regenerate **1**. The pK_a was determined from the plot of [quinuclidine] *vs.* [**1**][quinuclidinium]/[**3**] (Figure S16).

The concentrations of **1**, **3**, quinuclidine (B), and quinuclidinium (BH) were determined assuming mass balance as follows. At the wavelengths monitored, the absorbance due to B and BH are negligible and hence excluded. Equation 1 defines the initial absorbance at a specific wavelength, prior to any addition of base.

$$A_o = \varepsilon_{\mathbf{3}} b[\mathbf{3}]_o \quad (1)$$

Equation 2 defines the final absorbance after excess base has been added to fully convert **3** to **1**. The absorbance is equal to that of **1** prior to addition of acid to generate **3** *in situ*.

$$\mathrm{A_f} = \varepsilon_{\mathbf{1}} \mathrm{b}[\mathbf{1}]_\mathrm{f} \quad (2)$$

During the titration, the total concentration of iron is equal to the initial concentration of **3** and the final concentration of **1**, as described in equation 3. The subscript t denotes titration.

$$[\mathbf{1}]_\mathrm{f} = [\mathbf{3}]_\mathrm{o} = [\mathbf{3}]_\mathrm{t} + [\mathbf{1}]_\mathrm{t} \quad (3)$$

Likewise, the total concentration of base/conjugate acid at equilibrium is equal to the amount of base added ($[B]_x$), as described in equation 4.

$$[\mathrm{B}]_\mathrm{x} = [\mathrm{B}]_\mathrm{t} + [\mathrm{BH}]_\mathrm{t} \quad (4)$$

Assuming mass balance, the ratio of $[\mathbf{1}]_t/[\mathbf{3}]_t$ at a point in the titration can be described by equation 5.

$$\frac{\mathrm{A_t}-\mathrm{A_o}}{\mathrm{A_f}-\mathrm{A_t}} = \frac{\varepsilon_{\mathbf{3}} \mathrm{b}[\mathbf{3}]_\mathrm{t} + \varepsilon_{\mathbf{1}} \mathrm{b}[\mathbf{1}]_\mathrm{t} - \varepsilon_{\mathbf{3}} \mathrm{b}[\mathbf{3}]_\mathrm{o}}{\varepsilon_{\mathbf{1}} \mathrm{b}[\mathbf{1}]_\mathrm{f} - \varepsilon_{\mathbf{3}} \mathrm{b}[\mathbf{3}]_\mathrm{t} - \varepsilon_{\mathbf{1}} \mathrm{b}[\mathbf{1}]_\mathrm{t}} = \frac{\varepsilon_{\mathbf{3}}([\mathbf{3}]_\mathrm{t} - [\mathbf{3}]_\mathrm{o}) + \varepsilon_{\mathbf{1}}[\mathbf{1}]_\mathrm{t}}{\varepsilon_{\mathbf{1}}([\mathbf{1}]_\mathrm{f} - [\mathbf{1}]_\mathrm{t}) - \varepsilon_{\mathbf{3}}[\mathbf{3}]_\mathrm{t}} = \frac{\varepsilon_{\mathbf{1}}[\mathbf{1}]_\mathrm{t} - \varepsilon_{\mathbf{3}}[\mathbf{1}]_\mathrm{t}}{\varepsilon_{\mathbf{1}}[\mathbf{3}]_\mathrm{t} - \varepsilon_{\mathbf{3}}[\mathbf{3}]_\mathrm{t}} = \frac{[\mathbf{1}]_\mathrm{t}}{[\mathbf{3}]_\mathrm{t}} \quad (5)$$

Rearrangement of equation 5 gives equation 6.

$$[\mathbf{1}]_\mathrm{t} = [\mathbf{3}]_\mathrm{t} \frac{\mathrm{A_t}-\mathrm{A_o}}{\mathrm{A_f}-\mathrm{A_t}} \quad (6)$$

Combining equations 3 and 6 gives equation 7.

$$[\mathbf{1}]_\mathrm{t} = \frac{\frac{\mathrm{A_t}-\mathrm{A_o}}{\mathrm{A_f}-\mathrm{A_t}}[\mathbf{3}]_\mathrm{o}}{\frac{\mathrm{A_t}-\mathrm{A_o}}{\mathrm{A_f}-\mathrm{A_t}}+1} \quad (7)$$

At equilibrium, the concentration of **1** is equal to that of BH (equation 8).

$$[\mathbf{1}]_\mathrm{t} = [\mathrm{BH}]_\mathrm{t} \quad (8)$$

Combining equations 4 and 8 gives equation 9.

$$[\mathrm{B}]_\mathrm{t} = [\mathrm{B}]_\mathrm{x} - [\mathbf{1}]_\mathrm{t} \quad (9)$$

The equilibrium constant is defined by equation 10.

$$K = \frac{[\mathbf{1}]_t[BH]_t}{[\mathbf{3}]_t[B]_t} \quad (10)$$

Equation 10 can be rearranged to give equation 11.

$$K[B]_t = \frac{[\mathbf{1}]_t[BH]_t}{[\mathbf{3}]_t} \quad (11)$$

Thus, a plot of $[B]_t$ vs. $([\mathbf{1}]_t/[\mathbf{3}]_t)[BH]_t$ gives K. These parameters are given by equations 5, 7, and 9. The pK_a of **3** is then obtained by equation 12.

$$pK_a(\mathbf{3}) = pK_a(BH) - \log K \quad (12)$$

The absorbance was monitored at both 610 and 520 nm, and a total of 7 titrations were done, 3 of which were done in 0.1 M [^{n}Bu$_4$N]PF$_6$. The error is reported as ± 2σ. The pK_a of quinuclidine in acetonitrile is 19.51 (± 0.11).[13] Attempts to use other bases with similar pK_a's (DMAP, 2-bromo-phenol) resulted in loss of reversibility, possibly due to coordination of the base to the iron centers.

In a typical experiment, a 0.14 mM solution of **1** in MeCN was prepared in the glove-box, and 3 mL was transferred to an injectable screw-capped cuvette with a silicone septum (Starna). MeCN solutions of [DMAPH]OTf (42 mM), quinuclidine (245 mM), and TBD (178 mM) were also prepared and transferred to vials with a screw-capped septum. The reagents were stored under a blanket of Ar, and transferred to the cuvette via gas-tight syringe. After obtaining an initial optical spectrum of **1**, 1 equiv of acid was added, the cuvette inverted, and the spectrum of **3** recorded. The solution of **3** was titrated with quinuclidine (5-10 equiv per addition), which was added via gas-tight syringe, and the cuvette inverted once prior to acquisition of the optical spectrum. At the end of the titration, 9 equiv of TBD was added to ensure reversibility by monitoring the band at 526 nm. All titrations were complete within 5 min of addition of acid, and only those that had 95+ % conversion back to **1** were used in the analysis.

A pK_a of 20.6 ± 0.2 was obtained for **3**.

(13) Izutsu, K., *Acid-Base Dissociation Constants in Dipolar Aprotic Solvents*. Blackwell Scientific Publications: Oxford, 1990.

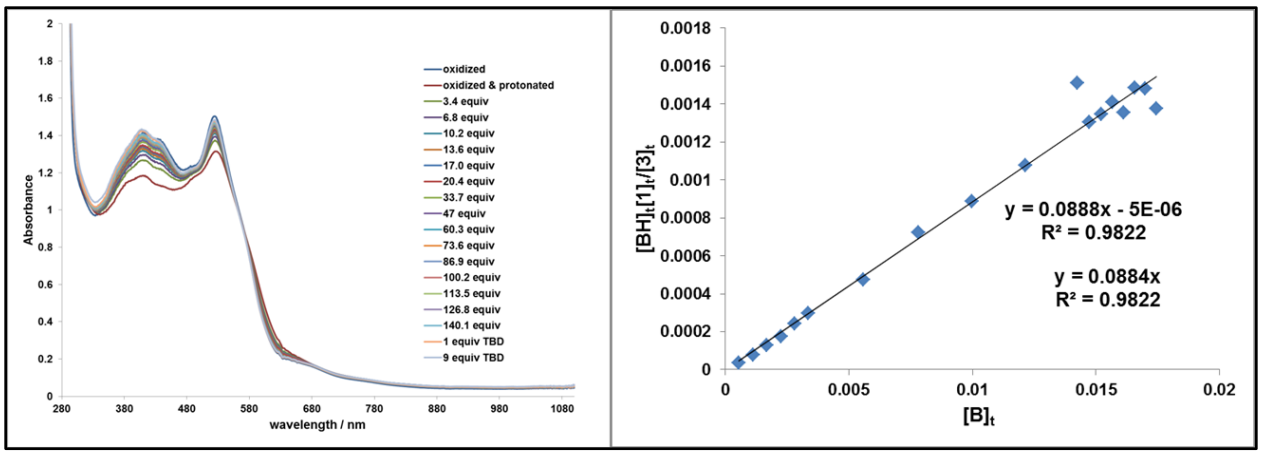

Figure S16. (left): UV-vis spectra of a titration of *in situ* generated **3** (MeCN) with quinuclidine; 98+ % conversion to **1** was observed. (right): Resulting plot of $[\text{quinuclidinium}]_t[\mathbf{1}]_t/[\mathbf{3}]_t$ vs. $[\text{quinuclidine}]_t$, from the changes observed at 610 nm.

pK_a Determination of [Fe_2S_2(^{Pr}bbimH)(^{Pr}bbim)](Et_4N)$_2$, 4.

Titrations to obtain the pK_a of **4** were monitored by ^{1}H NMR spectroscopy. As **4** can be irreversibly protonated, the pK_a of **4** was determined by titration of *in situ* generated **4** with a suitable base to generate **2**. The pK_a was determined from the plot of [DBU] vs. [**2**][DBUH$^+$]/[**4**] (Figure S17). The ArH resonance of **2** at 12.16 ppm was used to determine the concentration of **2** by integration against an internal standard of HMDS. As **4** is essentially NMR silent, the concentration of **4** was determined by mass balance (mixtures of **2** and **4** undergo slow exchange on the NMR time-scale). The concentration of protonated base was assumed to be the same as that of **2**, and the concentration of base determined by mass balance. The pK_a value obtained is an average from 3 independent runs (with a reported error of ± 2σ). No correction was applied to compensate for the degradation. Assuming that the degradation does not consume equivalents of acid or base and simply decreases the concentration of **2**/**4**, then compensating for degradation gives a pK_a that is 0.1 pK_a units smaller, within the error obtained. The pK_a of DBU in acetonitrile is 24.31.[14]

In a typical experiment, a stock 1.8 mM solution of **2** in d_3-MeCN was prepared. Neat HMDS was added (ca. 0.5 mM) as an internal standard, and 500 μL aliquots were transferred to 6 - 8 NMR tubes that were subsequently capped with a rubber septum and parafilmed. Solutions of acid (either [DMAPH]OTf or [pyH]OTf) and DBU were prepared in d_3-MeCN and transferred to vials with a screw-capped septum. The septum was punctured with a gas-tight syringe (to transfer solutions to NMR tubes) and a 5 mL syringe filled with N_2 (to ensure a positive pressure above the reagents). The ^{1}H NMR spectrum of **2** was recorded. One equiv of acid ([DMAPH]OTf or [pyH]OTf) was added to one NMR sample, the tube inverted once, DBU added (0.5 – 15 equiv), the tube inverted again, and inserted into the probe. The sample was shimmed, and the spectrum recorded. This process was repeated by adding different amounts of

(14) Kaljurand, I.; Kütt, A.; Sooväli, L.; Rodima, T.; Mäemets, V.; Leito, I.; Koppel, I. A., *J. Org. Chem.* **2005**, *70*, 1019.

DBU to the other samples. All data acquisition started within 2 min of acid addition. Exponential apodization along t1 (1.00 Hz) was applied to all spectra prior to manual phasing and baseline correction (Whittaker Smoother), and the integration regions was set equal for all spectra. A 10-15 % error is estimated on the integration. Despite working fast, ca. 5 – 15 % degradation was observed.

A pK_a of 24.7 ± 0.4 was obtained for **4**.

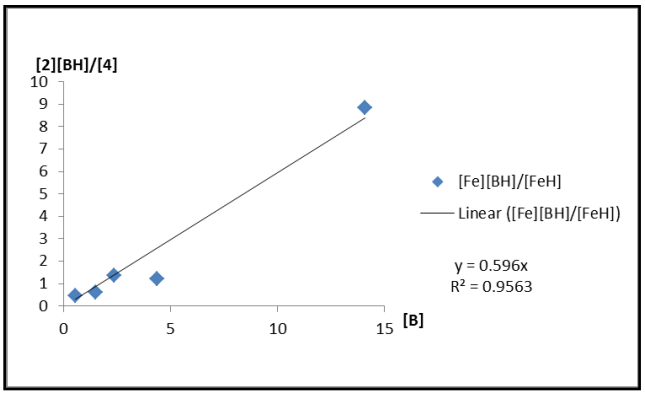

Figure S17. Plot of relative concentrations of [**2**][DBUH$^+$]/[**4**] vs. [DBU], obtained by measuring the concentration of **2** by ^{1}H NMR spectroscopy.

Electrochemistry

Cyclic voltammograms (CVs) were obtained using a CH Instruments 600D potentiostat, with a glassy carbon working electrode (0.3 cm diameter), $Ag/Ag(NO_3)$ reference electrode, and Pt auxiliary electrode. Unless noted, all electrochemical experiments were performed in the glove-box using MeCN with 0.25 M $^{n}Bu_4NPF_6$ electrolyte and 1 mM solutions of analyte at room temperature. CVs were either internally referenced to Fc/Fc^+ (0 V) by addition of Fc to the solution of analyte or externally referenced to Fc/Fc^+ by collecting the CV of Fc under identical conditions immediately before or after electrochemical experiments. Both methods gave identical and highly reproducible results. Reported reduction potentials are the average from several independent runs/scan-rates, and errors are reported as ± 2σ, unless otherwise noted.

In the presence of trace water (in the glove-box atmosphere), the diferric/mixed-valence couple shifts anodically, presumably due to an equilibrium between the deprotonated/protonated species (shifts of *ca*. 15 mV were observed). Upon addition of excess $^{t}BuN=P(pyrr)_3$ (pyrr = pyrrolyl), the diferric/mixed-valence couple shifts cathodically to its original value. CVs were only collected when addition of $^{t}BuN=P(pyrr)_3$ had no effect on the couple, ensuring no trace water.

The CVs of *in situ* generated **3** or **4** are complex, and suggest a ladder scheme, in which a second protonation is occurring and proton transfer amongst the electrochemically active species is fast on the CV timescale (see Figure S20). As a result of this, the peaks are broad and no longer reversible. The first anodic peak in the CV of **4** corresponds to oxidation to **3**, but the return cathodic wave associated with reduction of **3** to **4** is absent, as **4** is no longer present at the electrode. The reduction potential of **3** was thus estimated by measuring the shift in the oxidation peak of **2** upon addition of 1 equiv [pyH]OTf at a scan-rate of 1 V s^{-1}. The high scan-rate was to minimize subsequent protonation, and the peak position was taken to be where the derivative of the curve (current *vs.* potential) first reaches 0 (see Figure S21).

CVs collected at –20 ^{o}C were obtained by placing the electrochemical solutions in a custom-made aluminum block (that fits 20 mL scintillation vials and a thermocouple probe) and placing this in the glove-box cold-well which was chilled with a slurry of *o*-xylenes/CO_2. As the reduction potentials of the analyte, Fc/Fc^+, and $Ag/AgNO_3$ shift with temperature,[15] the CVs obtained at –20 ^{o}C were referenced to room temperature Fc/Fc^+ as follows. Immediately following the electrochemical experiments, the CV of Fc was collected at room temperature, and a temperature correction of +0.013 V (derived below) was applied.

The use of a non-isothermal cell to obtain reduction potentials at various temperatures is described in ref. 15. The temperature correction was obtained by using a non-isothermal cell to determine the $Ag/Ag(NO_3)$ potential relative to the room temperature Fc/Fc^+ couple. Outside the glove-box, a solution of electrolyte was added to an H-cell, with Fc, the working and reference electrodes in one compartment, and the $Ag/Ag(NO_3)$ reference electrode in the other. The Fc/Fc^+ potential referenced to $Ag/Ag(NO_3)$ was obtained at room temperature (0.087 V, 22 ^{o}C). The compartment that held the reference electrode was then cooled to –20 ^{o}C with an *o*-xylenes/CO_2 slurry, while the other was maintained at 22 ^{o}C with a water bath. The Fc/Fc^+ potential was again

(15) Kissinger, P. T.; Heineman, W. R., *Laboratory Techniques in Electroanalytical Chemistry Second Edition, Revised and Expanded*. 2 ed.; Marcel Dekker, Inc.: New York, 1996.

measured (0.100 V), indicative of a +0.013 V shift upon cooling for Ag/Ag(NO_3) relative to Fc at 22 ^{o}C.

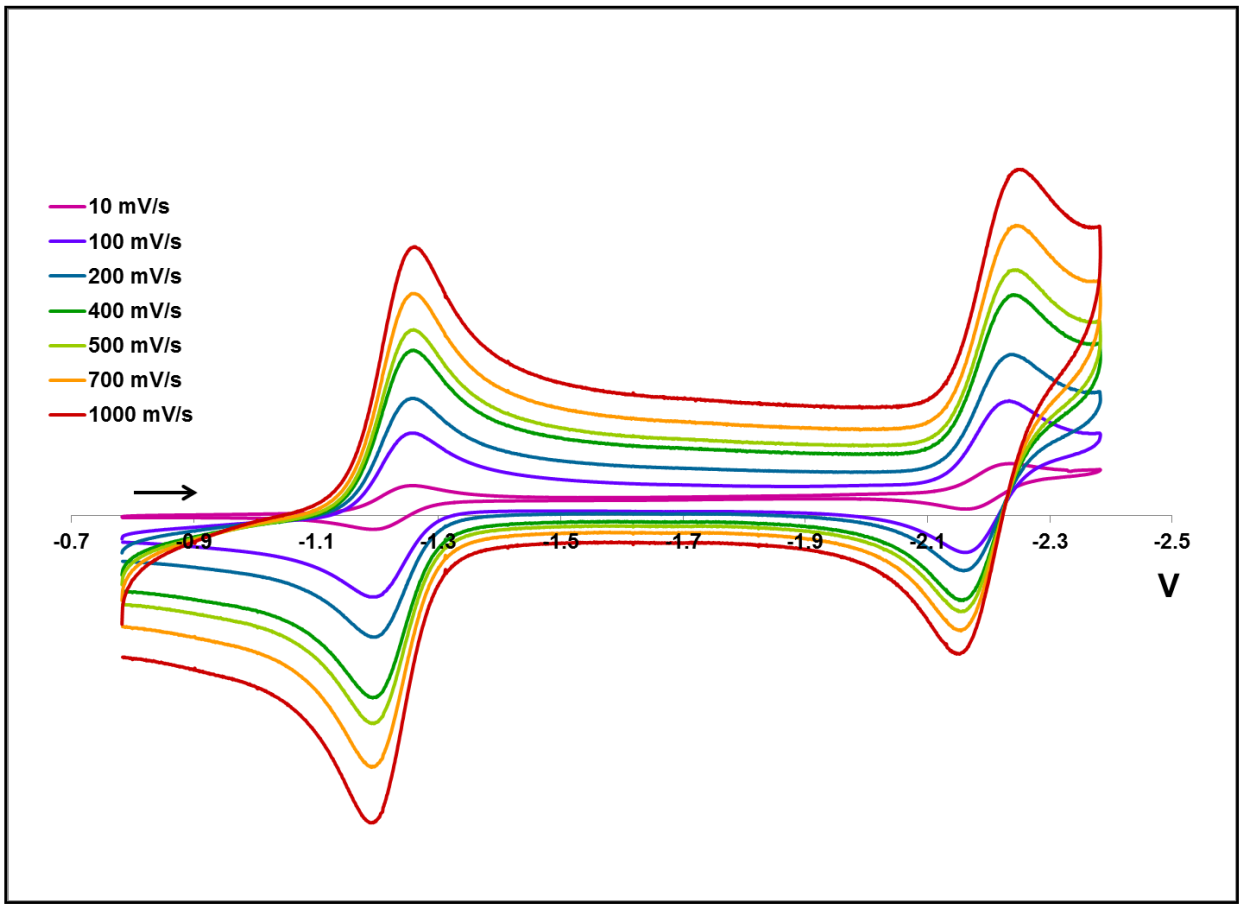

Figure S18. CVs of **1** (1 mM in 0.25 [^{n}Bu$_4$]PF_6, MeCN) obtained at different scan-rates. The arrow indicates the direction of the scan. Both the diferric/mixed-valence and mixed-valence/diferrous couples are electrochemically reversible (see Figure S19 and S20). The measured diferric/mixed-valence couple is at -1.225 ± 0.003 V and the mixed-valence/diferrous couple is at -2.198 ± 0.008 V vs. Fc/Fc^{+} (the error on these reduction potentials is given as ± 5σ). The large 0.973 V separation between the two couples is consistent with the observed stability of **2** towards redox disproportionation (K_c = {[Fe_2S_2(^{Pr}bbim)$_2$]$^{3-}$}^{2} / {[Fe_2S_2(^{Pr}bbim)$_2$]$^{2-}$ [Fe_2S_2(^{Pr}bbim)$_2$]$^{4-}$} = $10^{\Delta E/0.059\ V}$ = 3.1 x 10^{16}). CVs of **2** gave identical electrochemical behavior.

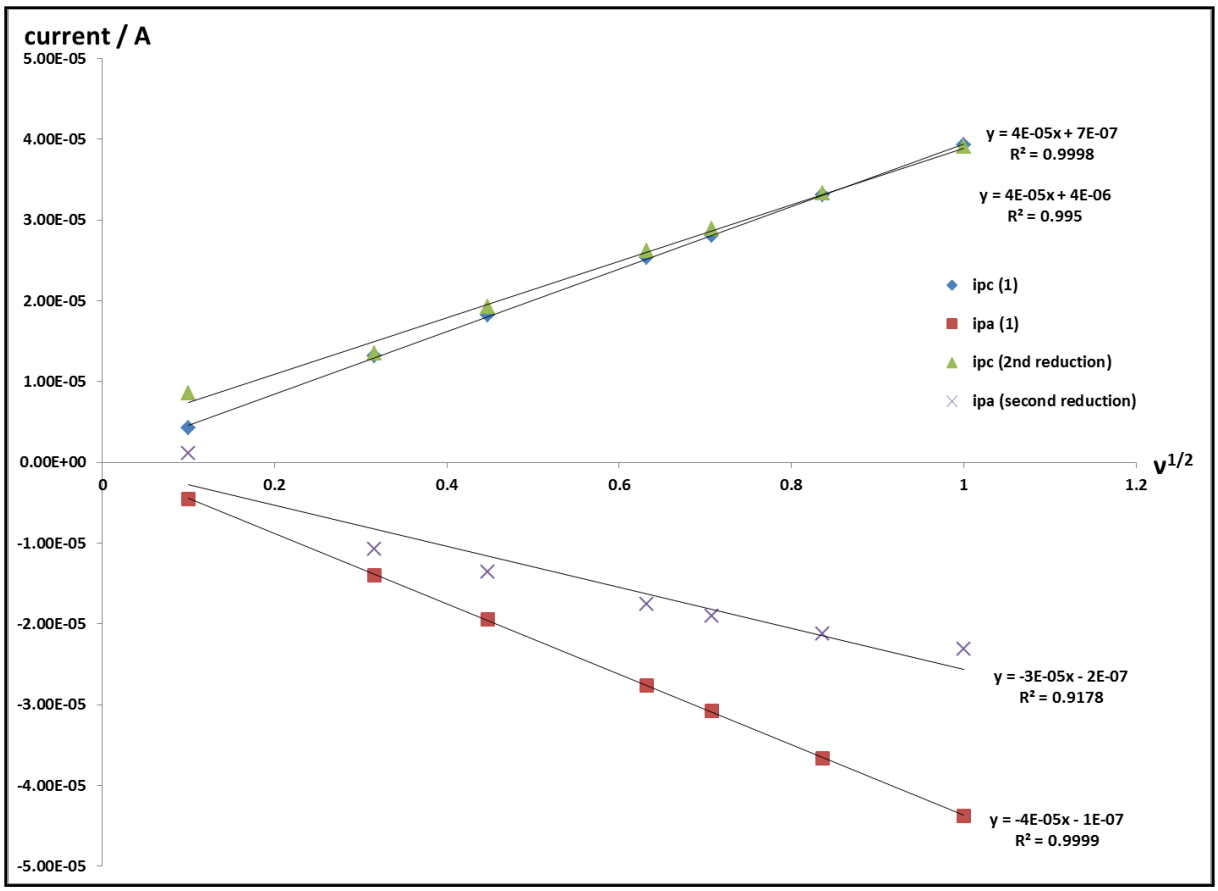

Figure S19. Plot of the square root of scan-rate versus current for the CVs of **1** (Figure S18)**.** The slope of the plot is equal to: (2.69 x 10^5)$n^{3/2}AD^{1/2}C$, where *n* is the number of electrons, A is the area of the electrode (cm^2), D is the diffusion coefficient (cm^2 s^{-1}), and C is the concentration (mol/mL). From this, the diffusion coefficient for the clusters is estimated to be *ca*. 3×10^{-6} cm^2 s^{-1}.

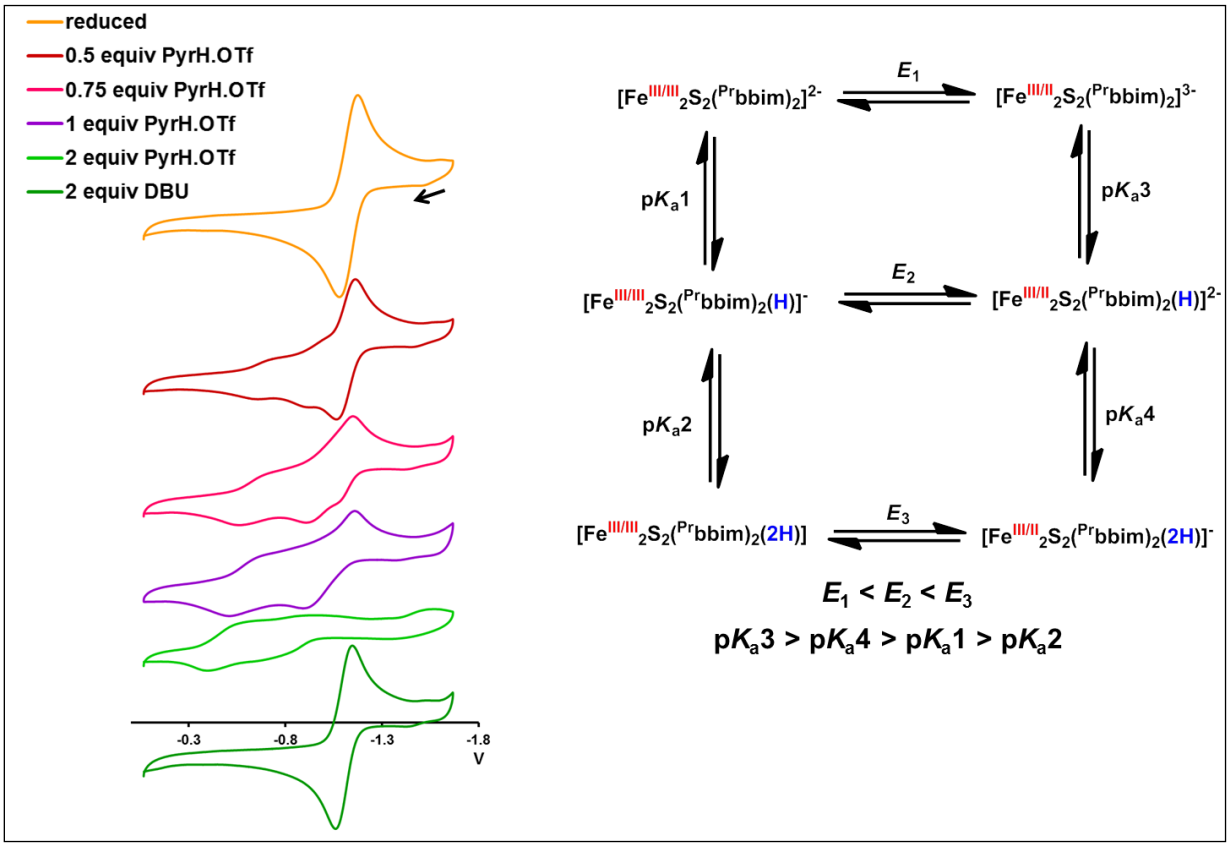

Figure S20. (left): Stacked CVs of **2** in the presence of increasing amounts of [pyH]OTf (0.5 – 2 equiv) and then 2 equiv of DBU. CVs were obtained at –20 °C at a scan-rate of 100 mV s^{-1} (1.0 mM **2**, 0.25 [^{n}Bu$_4$N]PF$_6$ in MeCN). The arrow indicates the start of the scan. (right): Ladder scheme indicating the proposed electro-chemically active species in solution, with the relative ordering of the pK_as and reduction potentials. With < 1 equiv acid, three oxidation peaks are observed, the most negative corresponding to the oxidation of **2** to **1**. The other redox events are attributed to **4** and a twice-protonated cluster. The observation of the twice-protonated cluster suggests that the **3** (generated at the electrode) serves as an acid to protonate **4**. DBU is not basic enough to fully deprotonate **4**, and as a result, the single redox event observed after addition of 2 equiv DBU is anodically shifted relative to that of **2**.[16] A similar situation has been observed in this system, whereby trace water shifts the potentials anodically. Note the ladder scheme drawn is a simplification, as one equiv of the conjugate base (py) is also present in the system, which can particulate in the proton transfer equilibria.

(16) Laviron, E.; Roullier, L., *J. Electroanal. Chem. Interfac.* **1985**, *186*, 1.

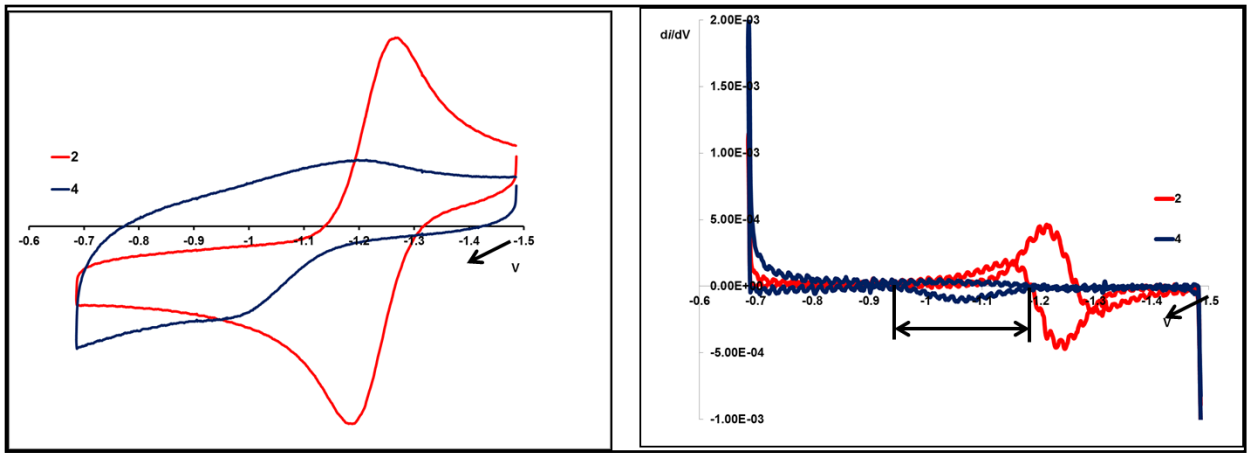

Figure S21. (left): Overlaid CVs of **2** (red) and **4** (blue), generated *in situ* from the addition of 1 equiv [pyH]OTf. The latter was taken immediately following addition of acid. Conditions: 1.0 mM cluster, 0.25 $[_n Bu_4]PF_6$ (MeCN), 1000 mV s^{-1} scan-rate, 22 ^oC. (right): derivative (of current *vs*. potential curve, see right curve) *vs*. potential of the CV of **2** and **4**. Assuming that in the absence of acid/base chemistry **4** is electrochemically reversible (*i.e.* similar peak-to-peak separation as **2**), then the shift in the oxidation peak (upon protonation) should approximate the shift in reduction potential upon protonation. Peak positions were taken to be where the derivative of the curve first reaches zero. Using this method, a shift of 0.245 ± 0.02 V was observed, corresponding to an reduction potential of –0.98 ± 0.02 V for **3**.

Double Mixing Stopped-Flow Kinetics

Rapid kinetic measurements were taken using a HI-TECH SCIENTIFIC CryoStopped-Flow System (SF-61DX2) capable of double-mixing, and equipped with a TC-61 temperature controller and a diode array detector. The stopped-flow system was controlled by the Kinetic Studio 2.20 software. The system was thermally equilibrated for 30-60 min before data acquisition at each temperature, and prior to kinetic runs, the stopped-flow was thoroughly flushed with dry MeCN.

All volumetric glassware and glass syringes employed were rinsed with dry MeCN in the glove-box prior to use. In the glove-box, MeCN solutions of **2** (0.74 mM), [DMAP-H]OTf (0.69 mM), and TEMPO (3.2, 6.8, 9.4, 12.4, and 16.9 mM) were prepared. Reagents and MeCN were loaded into gas-tight syringes (Hamilton or SGE), which were attached to gas-tight 2-way valves (SGE). The syringes were placed into individual Ziploc bags filled with glove-box atmosphere, removed from the glove-box, and immediately attached to the stopped-flow. The individual stopped-flow lines were rinsed with reagent prior to shots. The first two shots of every temperature/concentration combination were omitted.

Cluster **4** was prepared *in situ*, by mixing solutions of **2** and [DMAP-H]OTf. After a set delay time of 10 s, this solution was mixed with a solution of TEMPO, and 500 UV-vis spectra were recorded (over the course of 0.75, 1.5, 3.5, 7.5, 15, or 37.5 seconds). The initial TEMPO solution was diluted 2-fold, whereas the initial solution of **2** was diluted 4-fold. Four to six kinetic runs were done at each TEMPO concentration and temperature. Kinetic data were analyzed using SPECFIT. Typical spectra and kinetic fit are shown in Figure S22. The linear regression of k_{obs} versus [TEMPO] and the Eyring plot was done in Kaleidagraph, weighting each rate constant with its associated standard deviation. Standard errors were obtained from the plots, which were converted to standard deviation. Reported errors are double the fully propagated standard deviations, except that of the activation entropy, which is quadruple the fully propagated standard deviation.

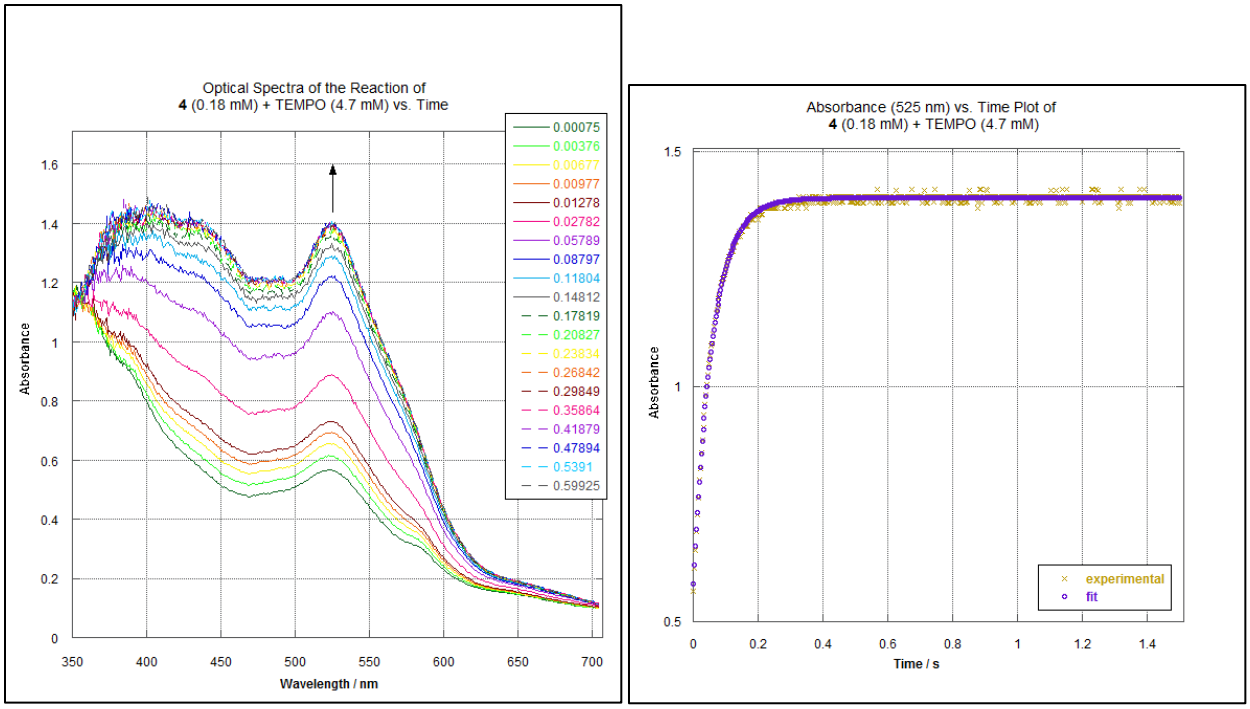

Figure S22. (left): Time evolution of UV-vis spectra of the reaction between **4** (0.35 mM; generated in the age-loop of the stopped-flow) and TEMPO (9.4 mM) over 1.5 s at 323 K in MeCN. (right): Match between the experimental and *pseudo*-first-order fit resulting from SPECFIT global analysis over the whole wavelength region (shown only for 525 nm).

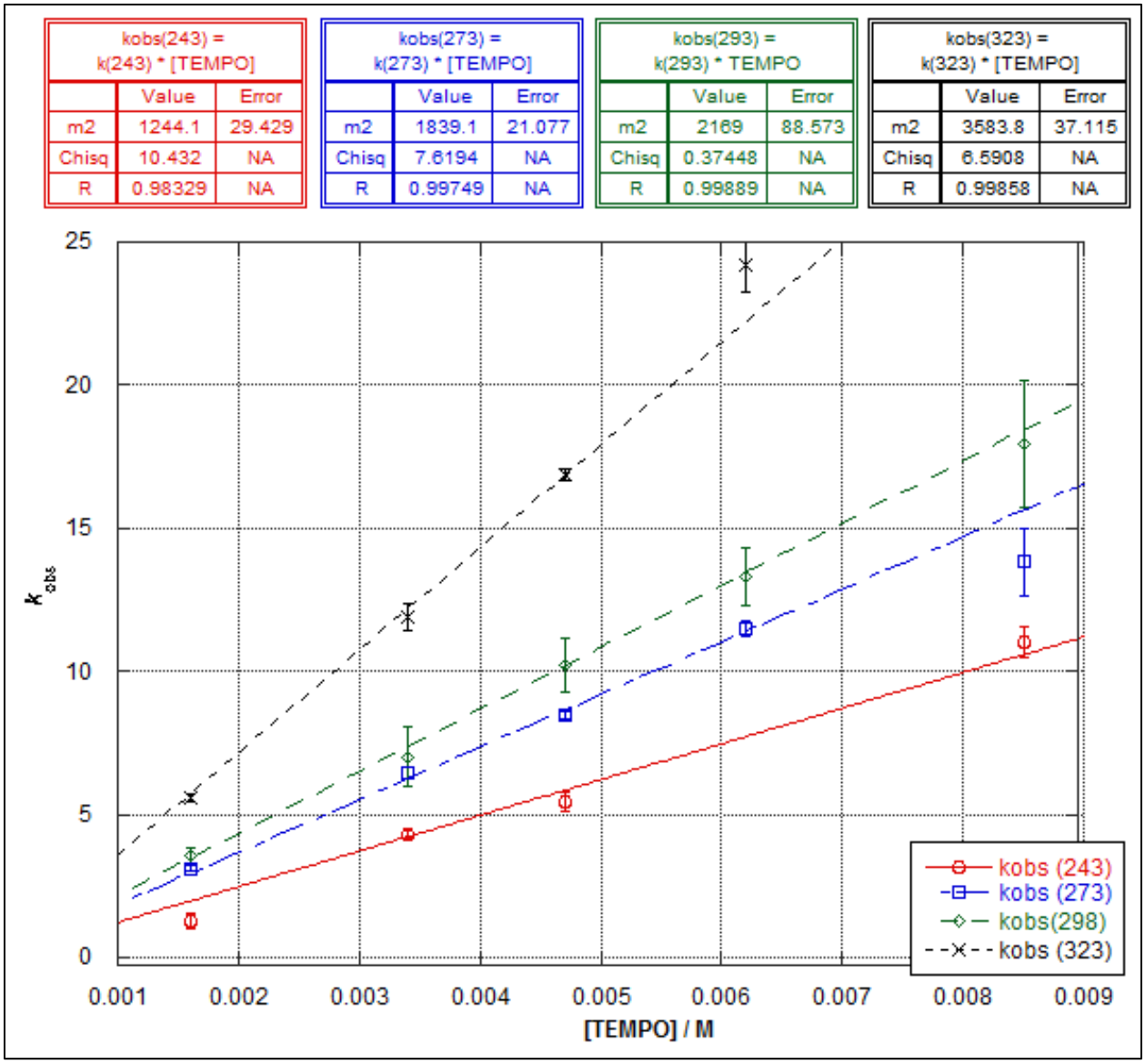

Figure S23. *Pseudo* first order plots of the reaction between **4** (0.1 mM, generated *in situ*) and excess TEMPO, obtained at different temperatures. The slope of each line gives the corresponding *k* for each temperature. At 298 K, $\Delta G^{\ddagger} = 12.9 \pm 0.3$ kcal mol^{-1}.

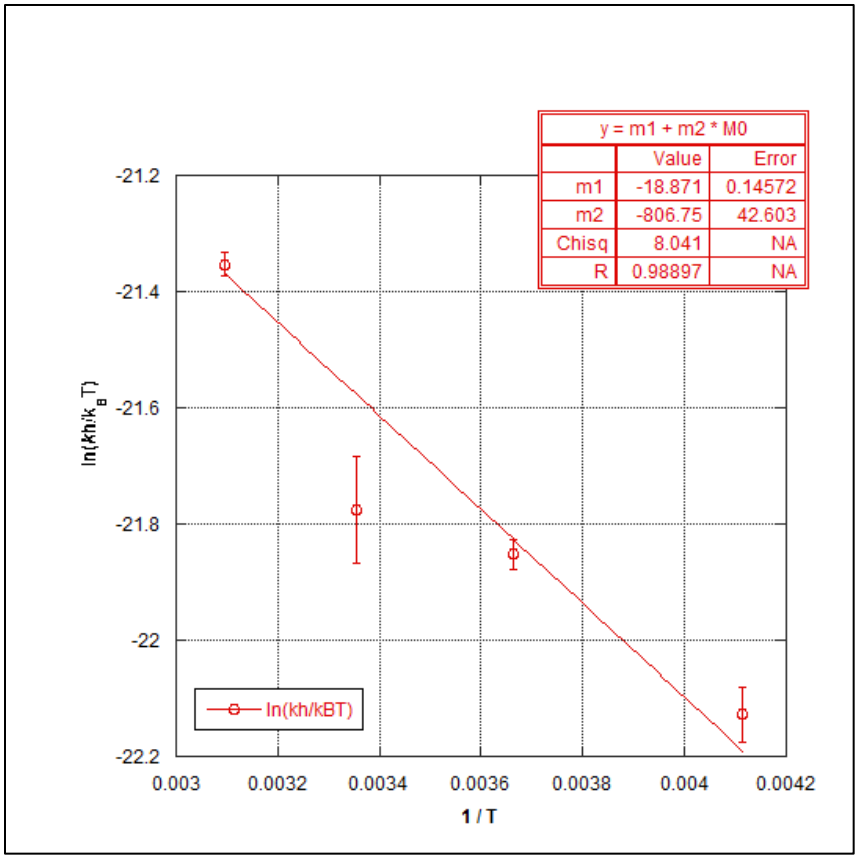

Figure S24. Eyring plot for the reaction of **4** with TEMPO. The following activation parameters are derived from the plot: $\Delta H^{\ddagger}$ = 1.6 ± 0.3 kcal mol^{-1}, $\Delta S^{\ddagger}$ = - 38 ± 2.4 cal K^{-1} mol^{-1}.

NMR monitoring of the decomposition of 3.

Cluster **3** decomposes to give mixtures of **1**, free ^{Pr}bbimH$_2$, and at least one paramagnetic iron-containing species that is soluble in MeCN, and insoluble dark solids. The relative amounts of the decomposition species varies, and is dependent on the solvent and acid employed as well as other variables. No isosbestic points are present when the decay is monitored by optical spectroscopy. The decomposition of **3** was monitored by ^{1}H NMR spectroscopy. The ratio of **1** to **3** was inferred from the position of the Ar*H* position that resonates at *ca*. 5.6 ppm. Mixtures of **1**/**3** give an average signal for each type of Ar-H resonance, and a plot of increasing **1**:**3** vs. chemical shift gives a straight line.

To a stirring solution of **1** (5.3 mg, 0.0048 mmol) in 1.27 mL d_3-MeCN (3.8 mM), 1 equiv of [DMAP-H]OTf was added (81 μL of a 60 mM solution in d_3-MeCN). The solution was transferred to an NMR tube, and ^{1}H NMR spectra collected at 10, 130, 270, and 500 min (solids were present for the latter 3 measurements). Both 1st and 2nd order plots give a straight line, with $t_{1/2}$ of *ca*. 4 h for a 3.8 mM solution.

NMR monitoring of the decomposition of 4.

Cluster **4** decomposes to give insoluble black solids as well as a soluble iron species (see Figure S25). Some of the resonances observed are consistent with formation of a monomeric (^{Pr}bbim)$_x$Fe(II) species (mixing solutions of ^{Pr}bbimTl$_2$, FeCl$_2$, and [Et$_4$N]Cl gives rise to a species whose ^{1}H NMR spectrum contains several paramagnetically shifted resonances, which overlap with those observed in the degradation of **4**). Though the decomposition products are not known, the decomposition is reproducible, both in terms of the NMR peaks observed and their integration (*vs.* an internal standard or the conjugate base of the acid used to generate **4**).

To a solution of **2** (0.0049 g, 0.0040 mmol) in 600 μL d_3-MeCN, 0.9 μL of HMDS was added. The solution was transferred to an NMR tube that was capped with a rubber septum and subsequently parafilmed. The ^{1}H NMR spectrum of **2** was obtained, and 1 equiv of quinuclidinium triflate (200 μL in d_3-MeCN) was added via gas-tight syringe. The tube was inverted twice and inserted into the probe. Spectra were obtained every 5 min for 98 min (starting 3 min after addition of acid). The decay was monitored by observing the growth of the resonance at 7.24 ppm, which after full decay of **4**, integrates to 2 protons per cluster. From this the $t_{1/2}$ is estimated to be *ca*. 20 min (0.5 mM solution).

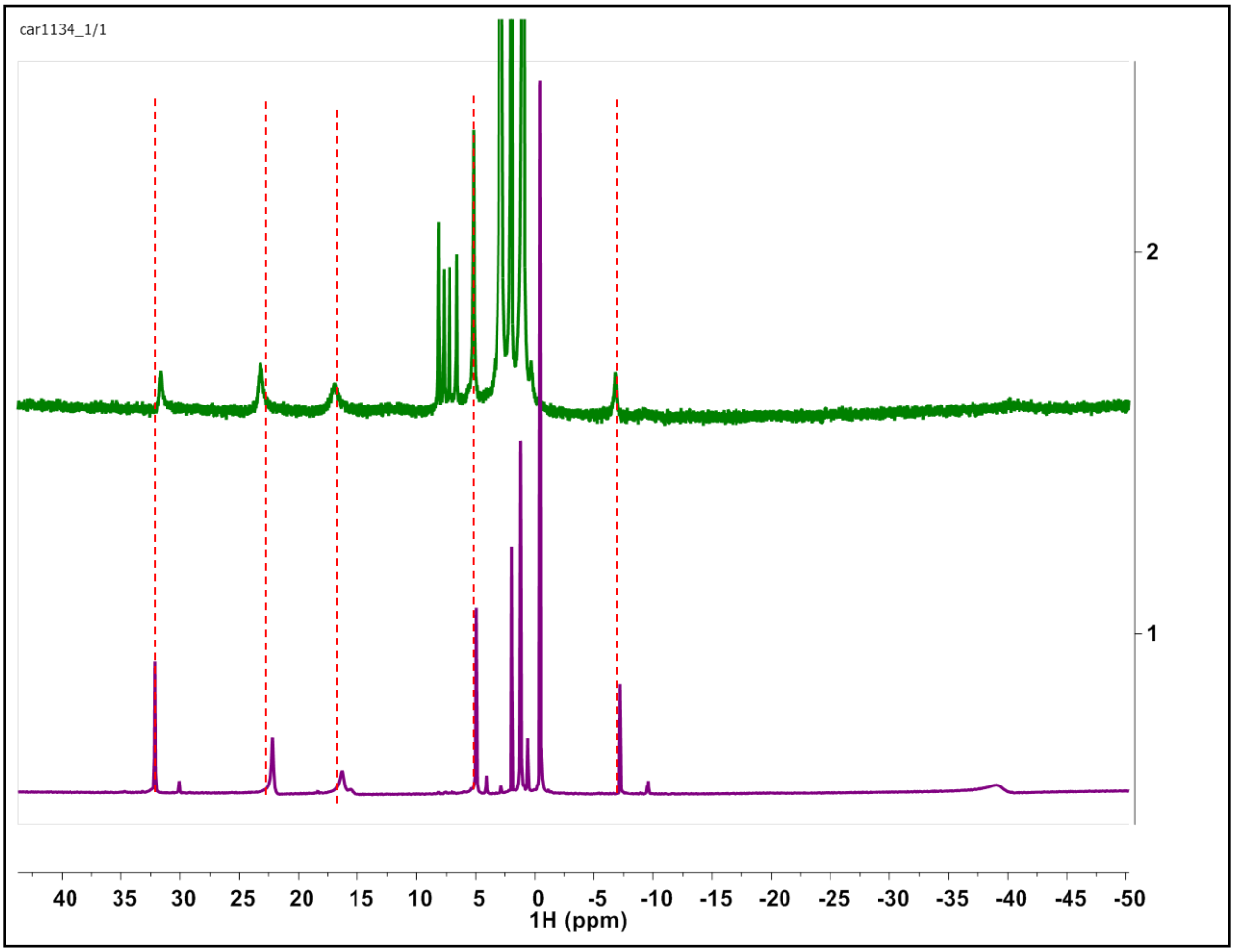

Figure S25. Stacked ^{1}H NMR spectra (MeCN-d_3) of (top): decomposition of **4**; (bottom): products formed upon mixing 2 ^{Pr}bbimTl$_2$, FeCl$_2$, and 2 (Et$_4$N)Cl. The dotted red lines indicate the similar resonances in both.

Table S1: Reduction potentials for various quinones in MeCN.

Quinone	Reduction Potential ($Q/SQ^{\cdot-}$) V *vs.* Fc/Fc^{+} [a]
2,5-dichloro-*p*-benzoquinone	-0.55
2,3,5,6-tetrachloro-*p*-benzoquinone	-0.36
2,3,5,6-tetramethyl-*p*-benzoquinone (duraquinone)	-1.23
p-benzoquinone	-0.89
2,5-di^{t}butyl-*p*-benzoquinone	-1.07
2,3-dimethoxy,5-methyl-*p*-benzoquinone (ubiquinone)	-1.04

[a] Reduction potentials obtained from the CV of the corresponding quinone in 0.25 M $[TBA]PF_6$ in MeCN at room temperature, with a 100 mV s^{-1} scan-rate.